

Towards Gluon PDFs in the Coulomb Gauge

Bill Good
07.05.2026

In Collaboration with:
Joshua Lin, Yong Zhao, Huey-Wen Lin



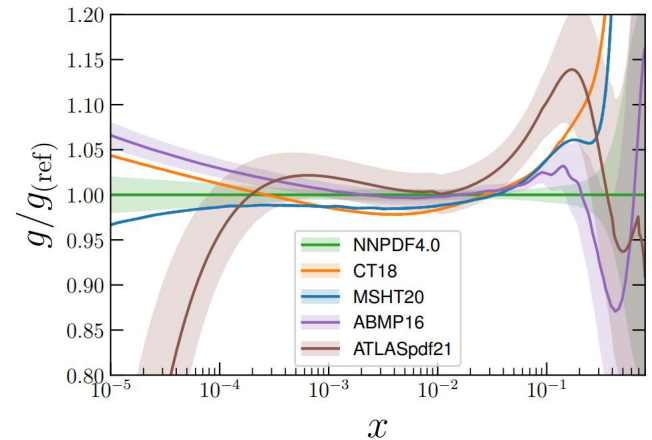
Introduction and Background

Introduction and Background

- Parton distribution functions (PDFs) provide the probability for a parton to carry a fraction x of the proton momentum, which is an important input for high energy scattering experiments

Introduction and Background

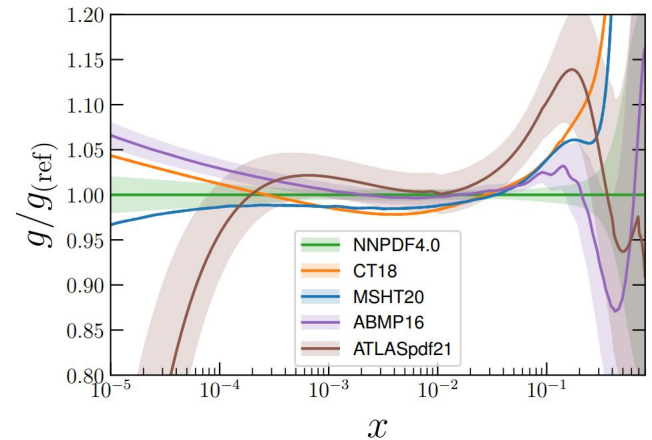
- Parton distribution functions (PDFs) provide the probability for a parton to carry a fraction x of the proton momentum, which is an important input for high energy scattering experiments
- Phenomenological (pheno.) studies of the gluon PDF have some difficulties in obtaining the PDF in the large- x region because of limited data



Amaroso, *et al.* (Snowmass) *Acta Physica Polonica. B*, 53, 12 (2023)

Introduction and Background

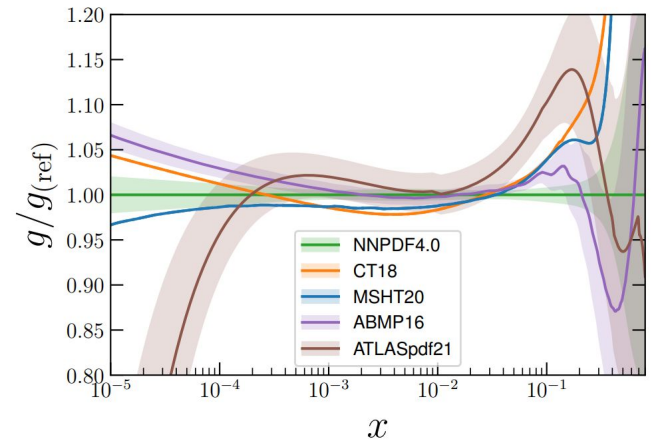
- Parton distribution functions (PDFs) provide the probability for a parton to carry a fraction x of the proton momentum, which is an important input for high energy scattering experiments
- Phenomenological (pheno.) studies of the gluon PDF have some difficulties in obtaining the PDF in the large- x region because of limited data
 - Ongoing and future experiments such as those at FNAL (HL-)LHC, LHeC, FCC(?), EIC, EicC will help reveal more information about the gluon PDFs



Amaroso, *et al.* (Snowmass) Acta Physica
Polonica. B, 53, 12 (2023)

Introduction and Background

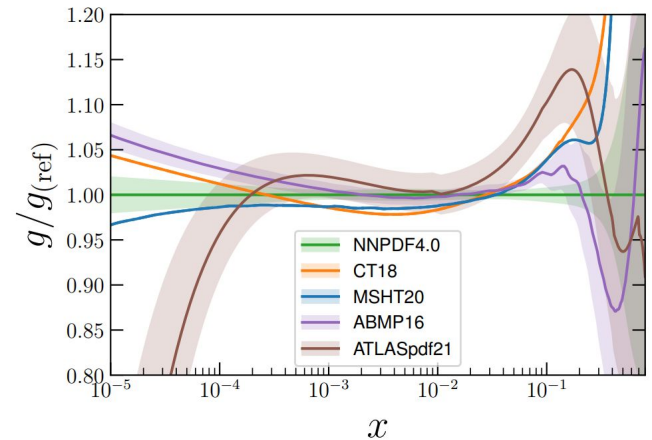
- Parton distribution functions (PDFs) provide the probability for a parton to carry a fraction x of the proton momentum, which is an important input for high energy scattering experiments
- Phenomenological (pheno.) studies of the gluon PDF have some difficulties in obtaining the PDF in the large- x region because of limited data
 - Ongoing and future experiments such as those at FNAL (HL-)LHC, LHeC, FCC(?), EIC, EicC will help reveal more information about the gluon PDFs
- LaMET and other lattice methods have provided some results for gluon PDFs but there is much statistical and systematic improvement left to be done



Amaroso, *et al.* (Snowmass) *Acta Physica Polonica. B*, 53, 12 (2023)

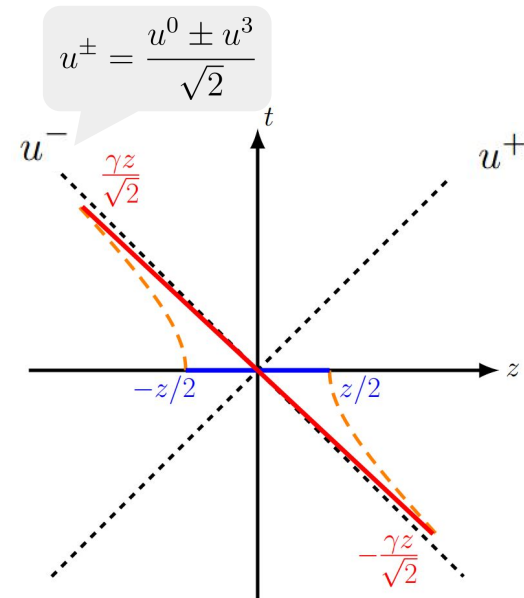
Introduction and Background

- Parton distribution functions (PDFs) provide the probability for a parton to carry a fraction x of the proton momentum, which is an important input for high energy scattering experiments
- Phenomenological (pheno.) studies of the gluon PDF have some difficulties in obtaining the PDF in the large- x region because of limited data
 - Ongoing and future experiments such as those at FNAL (HL-)LHC, LHeC, FCC(?), EIC, EicC will help reveal more information about the gluon PDFs
- LaMET and other lattice methods have provided some results for gluon PDFs but there is much statistical and systematic improvement left to be done
- Coulomb gauge PDFs promise to reduce statistical errors and in turn allow us to go to higher momenta, lower pion mass, etc.



Amaroso, *et al.* (Snowmass) *Acta Physica Polonica. B*, 53, 12 (2023)

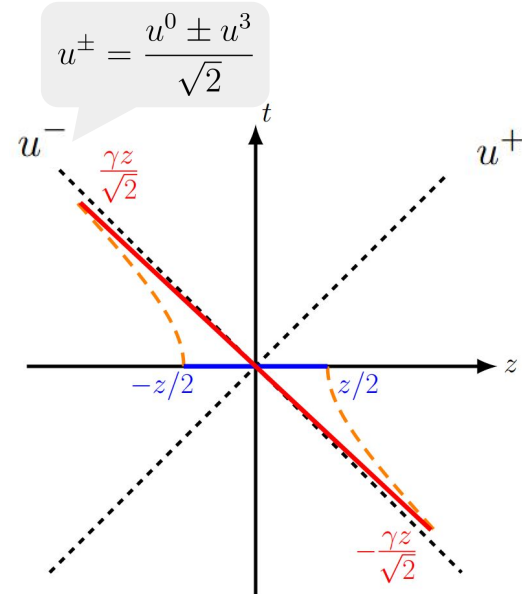
Light Cone Gluon PDFs



Light Cone Gluon PDFs

PDFs are formally defined by light-cone (LC) correlations of gluon field strength tensors:

$$g(x) = \frac{1}{xP^+} \int dz^- e^{ixP^+z^-} \langle P | F^{+\mu}(z^-) W(0, z^-) F_{\mu}^+(0) | P \rangle$$

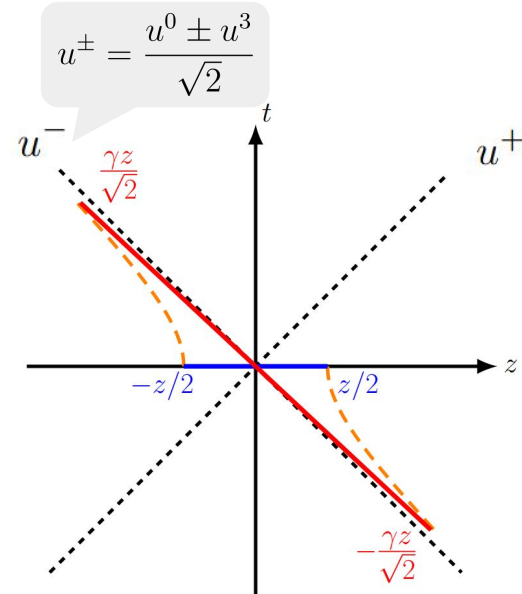


Light Cone Gluon PDFs

PDFs are formally defined by light-cone (LC) correlations of gluon field strength tensors:

$$g(x) = \frac{1}{xP^+} \int dz^- e^{ixP^+z^-} \langle P | F^{+\mu}(z^-) W(0, z^-) F_{\mu}^+(0) | P \rangle$$

With wilson line: $W(z, 0) = \mathcal{P} \exp \left[-ig \int_0^z dz' A^z(z') \right]$



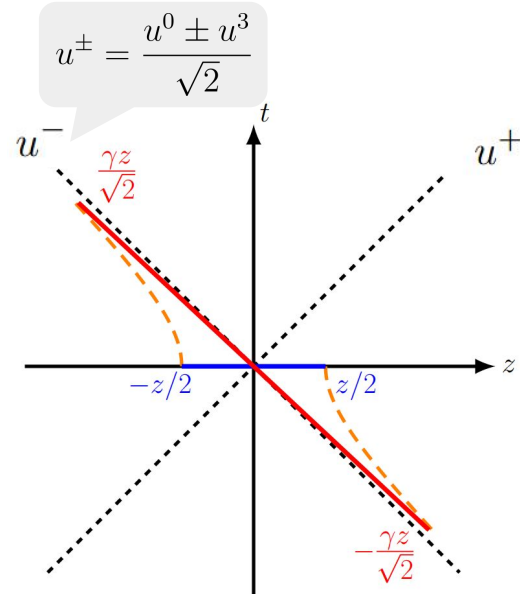
Light Cone Gluon PDFs

PDFs are formally defined by light-cone (LC) correlations of gluon field strength tensors:

$$g(x) = \frac{1}{xP^+} \int dz^- e^{ixP^+z^-} \langle P | F^{+\mu}(z^-) W(0, z^-) F_{\mu}^+(0) | P \rangle$$

With wilson line: $W(z, 0) = \mathcal{P} \exp \left[-ig \int_0^z dz' A^z(z') \right]$

Of course, the main idea behind LaMET is that we can only measure Euclidean correlators on the lattice, which naively approach the light-cone PDF in the infinite momentum limit



Light Cone Gluon PDFs

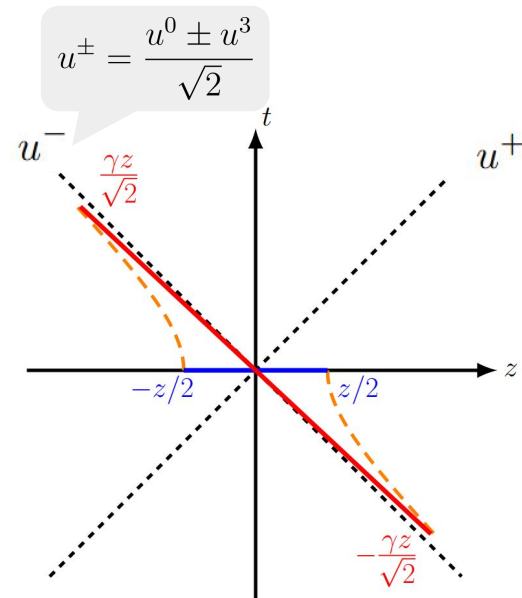
PDFs are formally defined by light-cone (LC) correlations of gluon field strength tensors:

$$g(x) = \frac{1}{xP^+} \int dz^- e^{ixP^+z^-} \langle P | F^{+\mu}(z^-) W(0, z^-) F_{\mu}^+(0) | P \rangle$$

With wilson line: $W(z, 0) = \mathcal{P} \exp \left[-ig \int_0^z dz' A^z(z') \right]$

Of course, the main idea behind LaMET is that we can only measure Euclidean correlators on the lattice, which naively approach the light-cone PDF in the infinite momentum limit

Though, non-commutativity of the UV and large momentum limits necessitate some perturbative matching relation to actually recover the light-cone PDF



Light Cone Gluon PDFs

PDFs are formally defined by light-cone (LC) correlations of gluon field strength tensors:

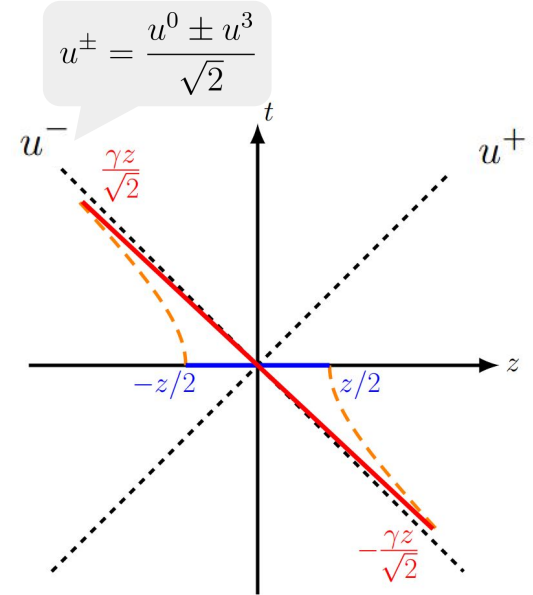
$$g(x) = \frac{1}{xP^+} \int dz^- e^{ixP^+z^-} \langle P | F^{+\mu}(z^-) W(0, z^-) F_{\mu}^+(0) | P \rangle$$

With wilson line: $W(z, 0) = \mathcal{P} \exp \left[-ig \int_0^z dz' A^z(z') \right]$

Of course, the main idea behind LaMET is that we can only measure Euclidean correlators on the lattice, which naively approach the light-cone PDF in the infinite momentum limit

Though, non-commutativity of the UV and large momentum limits necessitate some perturbative matching relation to actually recover the light-cone PDF

$$xg(x, \mu^2) = \int dy C_{gg} \left(\frac{x}{y}, \frac{\mu^2}{P_z^2} \right) y \tilde{g}(y, P_z) + C_{gq} \left(\frac{x}{y}, \frac{\mu^2}{P_z^2} \right) \tilde{q}(y, P_z) + \mathcal{O} \left(\frac{\Lambda_{\text{QCD}}^2}{(xP_z)^2}, \frac{\Lambda_{\text{QCD}}^2}{((1-x)P_z)^2} \right)$$



Euclidean Gluon Quasi-/Pseudo-PDFs

Euclidean Gluon Quasi-/Pseudo-PDFs

- The number of indices in the LC PDF operator leave some freedom of choice in the quasi-PDF operator

$$O_g^{\text{LC}}(z^-) = F^{+\mu}(z^-)W(z, 0)F_{\mu}^+(0)$$

Euclidean Gluon Quasi-/Pseudo-PDFs

- The number of indices in the LC PDF operator leave some freedom of choice in the quasi-PDF operator

$$O_g^{\text{LC}}(z^-) = F^{+\mu}(z^-)W(z, 0)F_{\mu}^+(0)$$

- We have found that the following works the best on the lattice:

$$O_g(z) = F^{ti}(z)W(z, 0)F_i^t(0) - F^{ij}(z)W(z, 0)F_{ij}(0)$$

Balitsky, *et al.*, PLB 808:135621 (2020)
WG, *et al.* JPG 52:035105(3) (2025)
WG, *et al.* PLB 872:140067 (2026)

Euclidean Gluon Quasi-/Pseudo-PDFs

- The number of indices in the LC PDF operator leave some freedom of choice in the quasi-PDF operator

$$O_g^{\text{LC}}(z^-) = F^{+\mu}(z^-)W(z, 0)F_{\mu}^+(0)$$

- We have found that the following works the best on the lattice:

$$O_g(z) = F^{ti}(z)W(z, 0)F_i^t(0) - F^{ij}(z)W(z, 0)F_{ij}(0)$$

Balitsky, *et al.*, PLB 808:135621 (2020)
WG, *et al.* JPG 52:035105(3) (2025)
WG, *et al.* PLB 872:140067 (2026)

- There has been a lot of progress in gluon PDFs from the lattice, but we there is much left to be desired in terms of statistical and systematic precision:

Euclidean Gluon Quasi-/Pseudo-PDFs

- The number of indices in the LC PDF operator leave some freedom of choice in the quasi-PDF operator

$$O_g^{\text{LC}}(z^-) = F^{+\mu}(z^-)W(z, 0)F_{\mu}^+(0)$$

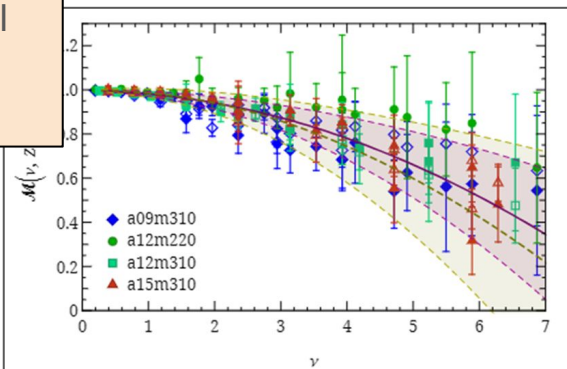
- We have found that the following works the best on the lattice: Balitsky, et al., PLB 808:135621 (2020)

$$O_g(z) = F^{ti}(z)W(z, 0)F_i^t(0) - F^{ij}(z)W(z, 0)F_{ij}(0)$$

WG, et al. JPG 52:035105(3) (2025)
WG, et al. PLB 872:140067 (2026)

- There has been a lot of progress in gluon PDFs from the lattice, but we there is much left to be desired in terms of statistical and systematic precision:

[MSULat] First physical continuum lattice nucleon gluon PDFs



Euclidean Gluon Quasi-/Pseudo-PDFs

- The number of indices in the LC PDF operator leave some freedom of choice in the quasi-PDF operator

$$O_g^{LC}(z^-) = F^{+\mu}(z^-)W(z, 0)F_\mu^+(0)$$

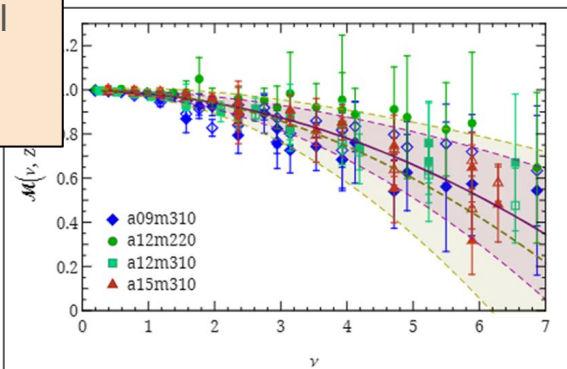
- We have found that the following works the best on the lattice: Balitsky, et al., PLB 808:135621 (2020)

$$O_g(z) = F^{ti}(z)W(z, 0)F_i^t(0) - F^{ij}(z)W(z, 0)F_{ij}(0)$$

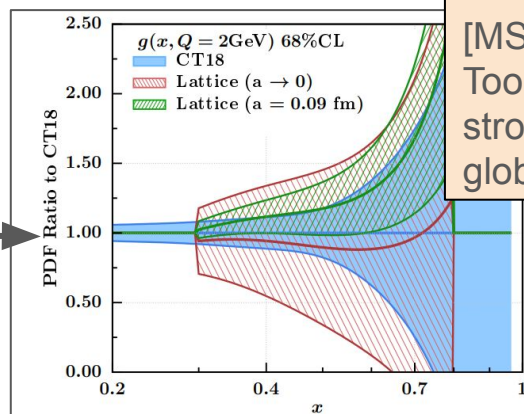
WG, et al. JPG 52:035105(3) (2025)
WG, et al. PLB 872:140067 (2026)

- There has been a lot of progress in gluon PDFs from the lattice, but there is much left to be desired in terms of statistical and systematic precision:

[MSULat] First physical continuum lattice nucleon gluon PDFs



PRD 108:014508(1), (2023)



[MSULat+CTEQ] Too noisy to strongly impact global fit arXiv:2502.10630

Euclidean Gluon Quasi-/Pseudo-PDFs

- The number of indices in the LC PDF operator leave some freedom of choice in the quasi-PDF operator

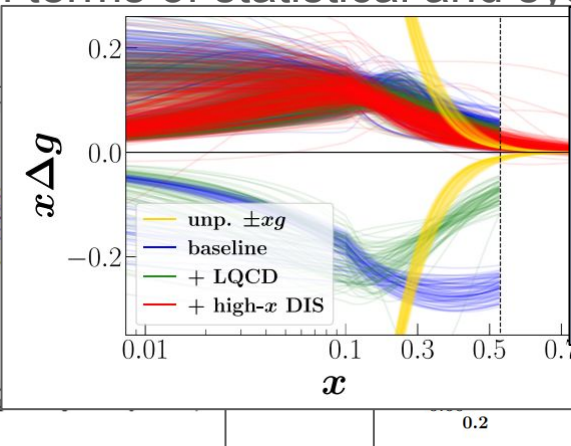
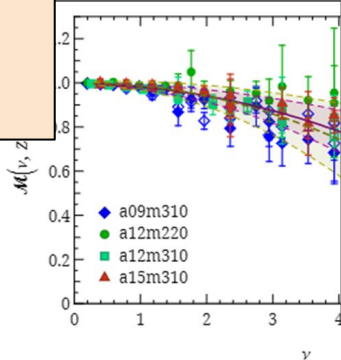
$$O_g^{\text{LC}}(z^-) = F^{+\mu}(z^-)W(z, 0)F_\mu^+(0)$$

- We have found that the following works the best on the lattice: Balitsky, et al., PLB 808:135621 (2020)
WG, et al. JPG 52:035105(3) (2025)
WG, et al. PLB 872:140067 (2026)

$$O_g(z) = F^{ti}(z)W(z, 0)F_i^t(0) - F^{ij}(z)W(z, 0)F_{ij}(0)$$

- There has been a lot of progress in gluon PDFs from the lattice, but there is much left to be desired in terms of statistical and systematic precision:

[MSULat] First physical continuum lattice nucleon gluon PDFs



[Hadstruc+JAM] Gluon helicity sign problem “solved”

PRD 109:036031(3), (2024)
PRL 133:161901(16), (2024)

10630

Euclidean Gluon Quasi-/Pseudo-PDFs

- The number of indices in the LC PDF operator leave some freedom of choice in the quasi-PDF operator

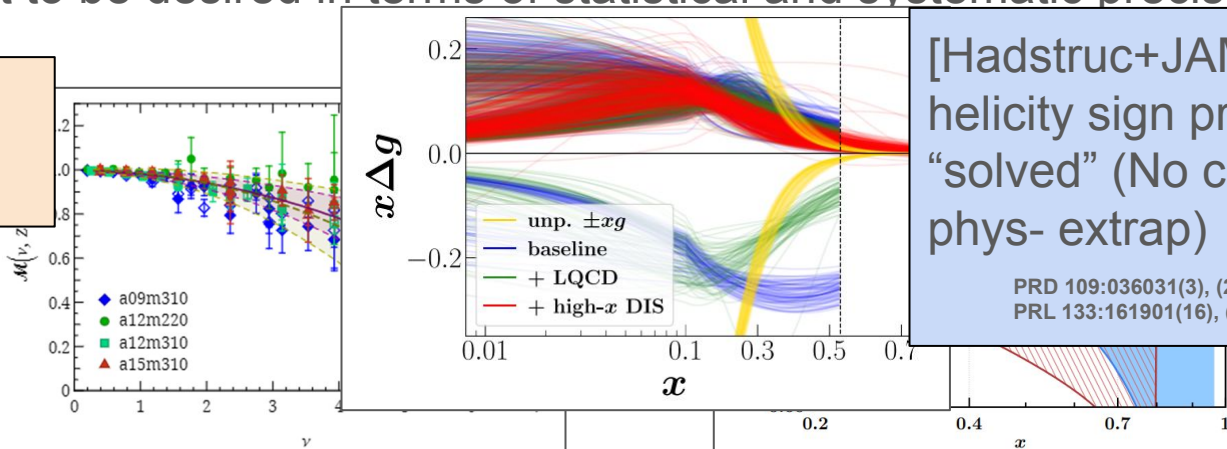
$$O_g^{\text{LC}}(z^-) = F^{+\mu}(z^-)W(z, 0)F_\mu^+(0)$$

- We have found that the following works the best on the lattice: Balitsky, et al., PLB 808:135621 (2020)
WG, et al. JPG 52:035105(3) (2025)
WG, et al. PLB 872:140067 (2026)

$$O_g(z) = F^{ti}(z)W(z, 0)F_i^t(0) - F^{ij}(z)W(z, 0)F_{ij}(0)$$

- There has been a lot of progress in gluon PDFs from the lattice, but there is much left to be desired in terms of statistical and systematic precision:

[MSULat] First physical continuum lattice nucleon gluon PDFs



[Hadstruc+JAM] Gluon helicity sign problem “solved” (No cont.-phys- extrap)

PRD 109:036031(3), (2024)
PRL 133:161901(16), (2024)

PRD 108:014508(1), (2023)

10630

Euclidean Gluon Quasi-/Pseudo-PDFs

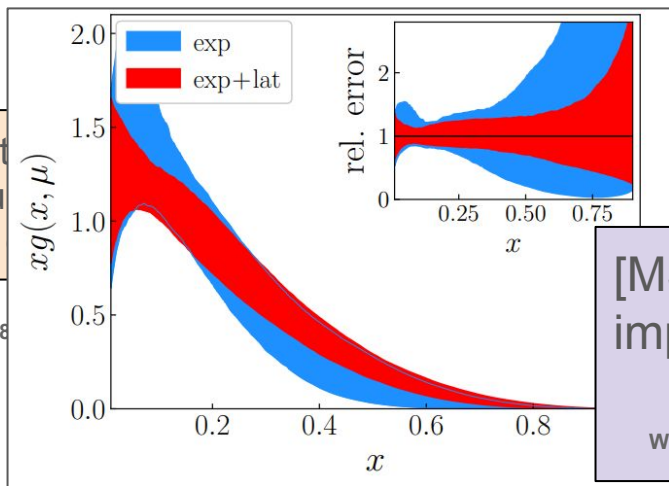
- The number of indices in the LC PDF operator leave some freedom of choice in the quasi-PDF operator

$$O_g^{\text{LC}}(z^-) = F^{+\mu}(z^-)W(z, 0)F_\mu^+(0)$$

- We have found that the following works the best on the lattice: Balitsky, et al., PLB 808:135621 (2020)
WG, et al. JPG 52:035105(3) (2025)
WG, et al. PLB 872:140067 (2026)

$$O_g(z) = F^{ti}(z)W(z, 0)F_i^t(0) - F^{ij}(z)W(z, 0)F_{ij}(0)$$

- There has been a lot of progress in gluon PDFs from the lattice, but we there



ms of statistical and systematic precision:

[Hadstruc+JAM] Gluon helicity sign problem “solved” (No cont.-phys- extrap)

PRD 109:036031(3), (2024)
PRL 133:161901(16), (2024)

[MSULat+JAM] Strong impact on pion gluon PDF

WG, et al. arXiv 2507.22730 (2025)

Euclidean Gluon Quasi-/Pseudo-PDFs

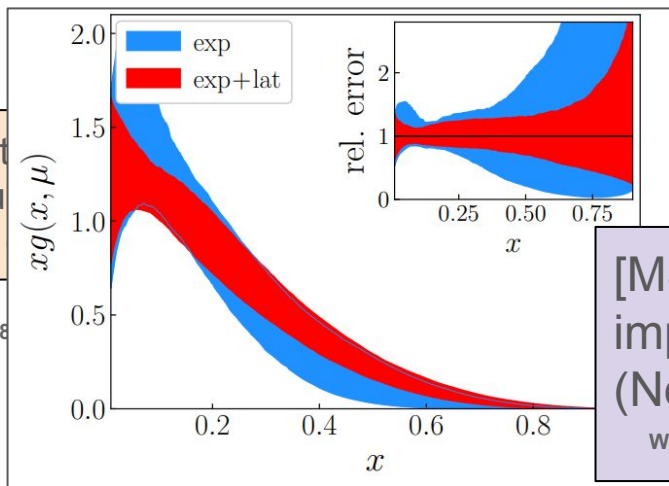
- The number of indices in the LC PDF operator leave some freedom of choice in the quasi-PDF operator

$$O_g^{\text{LC}}(z^-) = F^{+\mu}(z^-)W(z, 0)F_\mu^+(0)$$

- We have found that the following works the best on the lattice: Balitsky, et al., PLB 808:135621 (2020)
WG, et al. JPG 52:035105(3) (2025)
WG, et al. PLB 872:140067 (2026)

$$O_g(z) = F^{ti}(z)W(z, 0)F_i^t(0) - F^{ij}(z)W(z, 0)F_{ij}(0)$$

- There has been a lot of progress in gluon PDFs from the lattice, but we there



ms of statistical and systematic precision:

[Hadstruc+JAM] Gluon helicity sign problem “solved” (No cont.-phys- extrap)

PRD 109:036031(3), (2024)
PRL 133:161901(16), (2024)

[MSULat+JAM] Strong impact on pion gluon PDF (No cont.-phys- extrap)

WG, et al. arXiv 2507.22730 (2025)

10630

Euclidean Gluon Quasi-/Pseudo-PDFs

- The number of indices in the LC PDF operator leave some freedom of choice in the quasi-PDF operator

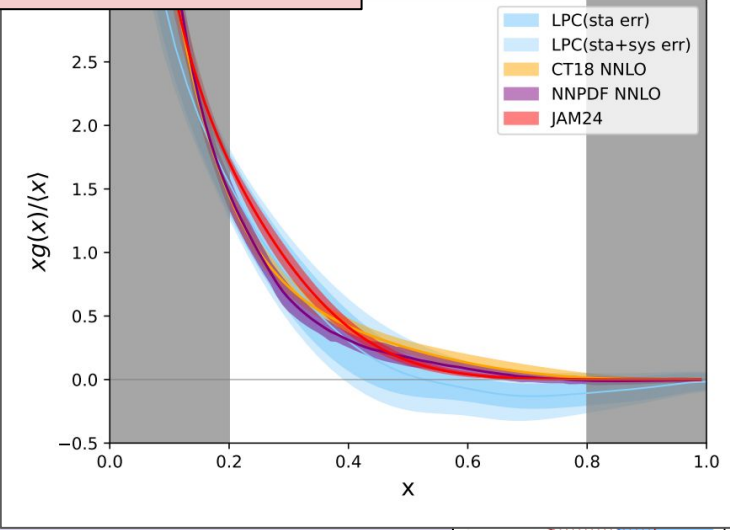
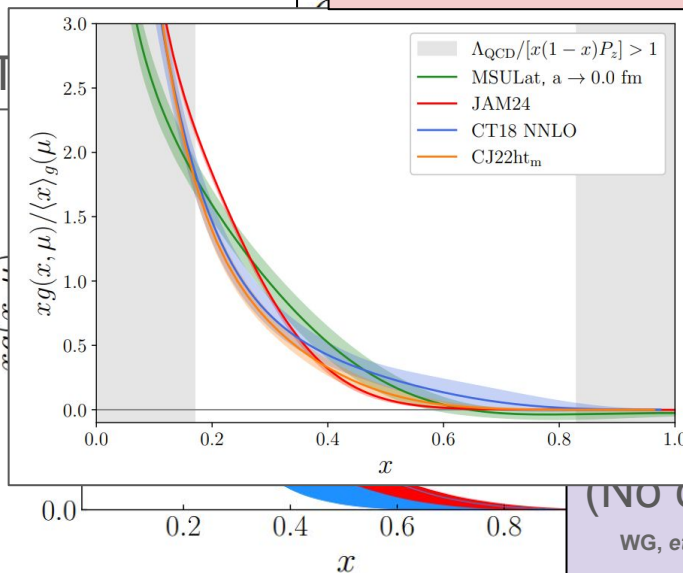
[MSULat and LPC] Continuum gluon PDFs from LaMET with self-renormalization

- We have found

NieMiera, et al. arXiv 2510.17758 Chen, et al. arXiv 2510.26425

the lattice:

Balitsky, et al., PLB 808:135621 (2020)
 WG, et al. JPG 52:035105(3) (2025)
 172:140067 (2026)



[MSULat continuum nucleon]

PRD 108:014508

there

n:
] Gluon
 blem
 nt.-

10630

WG, et al. arXiv 2507.22730 (2025)

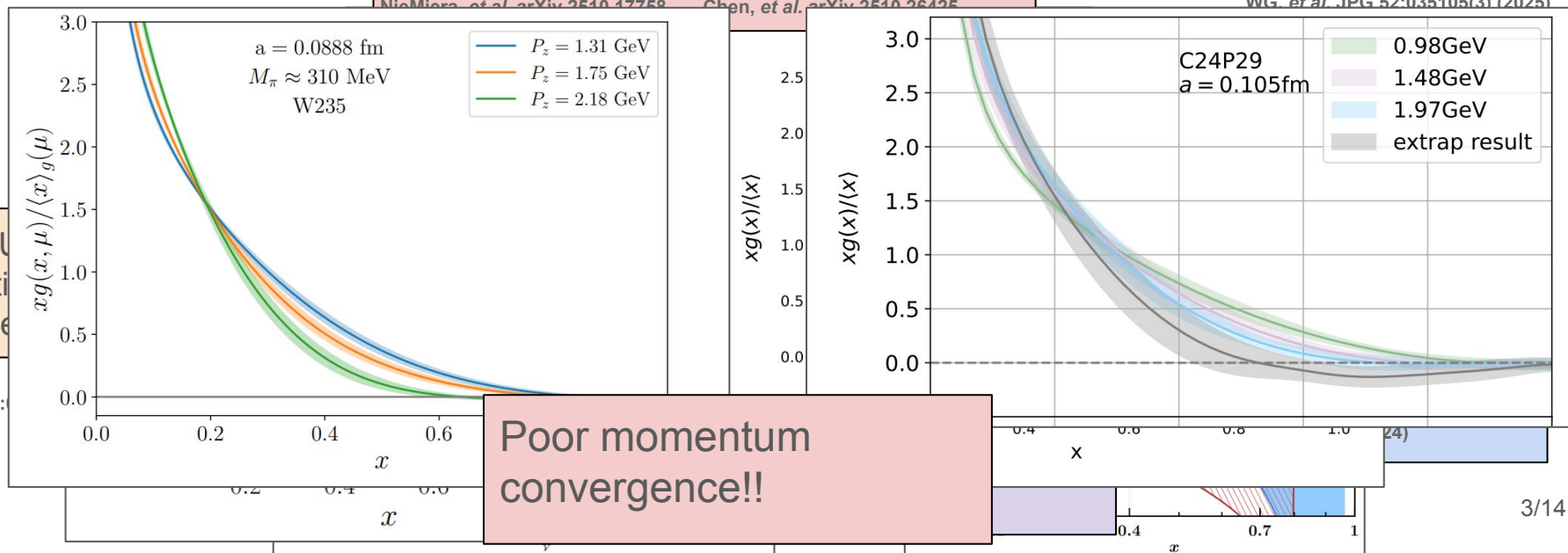
Euclidean Gluon Quasi-/Pseudo-PDFs

- The number of indices in the LC PDF operator leave some freedom of choice in the quasi-PDF operator

[MSULat and LPC] Continuum gluon PDFs from LaMET with self-renormalization

- We have found

the lattice: Balitsky, et al., PLB 808:135621 (2020)
WG, et al. JPG 52:035105(3) (2025)



Coulomb Gauge to the Rescue

Coulomb Gauge to the Rescue

- The self-energy of the Wilson line in the gauge invariant quasi-PDF operators causes the signal to noise ratio to decay exponentially at long distances

$$h_{\text{GI}}^{\text{B}}(z, P_z) = \langle P_z | \bar{\psi}(z) \gamma_t W(z, 0) \psi(0) | P_z \rangle \sim e^{-\delta m z}$$

Coulomb Gauge to the Rescue

- The self-energy of the Wilson line in the gauge invariant quasi-PDF operators causes the signal to noise ratio to decay exponentially at long distances

$$h_{\text{GI}}^{\text{B}}(z, P_z) = \langle P_z | \bar{\psi}(z) \gamma_t W(z, 0) \psi(0) | P_z \rangle \sim e^{-\delta m z}$$

- So, who needs gauge invariance anyway?

Coulomb Gauge to the Rescue

- The self-energy of the Wilson line in the gauge invariant quasi-PDF operators causes the signal to noise ratio to decay exponentially at long distances

$$h_{\text{GI}}^{\text{B}}(z, P_z) = \langle P_z | \bar{\psi}(z) \gamma_t W(z, 0) \psi(0) | P_z \rangle \sim e^{-\delta m z}$$

- So, who needs gauge invariance anyway? In the quark case, it has been shown that (a new) factorization holds and the signal is improved at long distances at large distances when we use Coulomb gauge (CG) operators

Coulomb Gauge to the Rescue

- The self-energy of the Wilson line in the gauge invariant quasi-PDF operators causes the signal to noise ratio to decay exponentially at long distances

$$h_{\text{GI}}^{\text{B}}(z, P_z) = \langle P_z | \bar{\psi}(z) \gamma_t W(z, 0) \psi(0) | P_z \rangle \sim e^{-\delta m z}$$

- So, who needs gauge invariance anyway? In the quark case, it has been shown that (a new) factorization holds and the signal is improved at long distances at large distances when we use Coulomb gauge (CG) operators

$$h_{\text{CG}}^{\text{B}}(z, P_z) = \langle P_z | \bar{\psi}(z) \gamma_t \psi(0) |_{\nabla \cdot \vec{A}=0} | P_z \rangle$$

Gao, et al. PRD 109(0):094506 (2024)

Coulomb Gauge to the Rescue

- The self-energy of the Wilson line in the gauge invariant quasi-PDF operators causes the signal to noise ratio to decay exponentially at long distances

$$h_{\text{GI}}^{\text{B}}(z, P_z) = \langle P_z | \bar{\psi}(z) \gamma_t W(z, 0) \psi(0) | P_z \rangle \sim e^{-\delta m z}$$

- So, who needs gauge invariance anyway? In the quark case, it has been shown that (a new) factorization holds and the signal is improved at long distances at large distances when we use Coulomb gauge (CG) operators

$$h_{\text{CG}}^{\text{B}}(z, P_z) = \langle P_z | \bar{\psi}(z) \gamma_t \psi(0) |_{\nabla \cdot \vec{A}=0} | P_z \rangle$$

Gao, et al. PRD 109(0):094506 (2024)

- Rapid progress has been made for CG in the quark case

Coulomb Gauge to the Rescue

- The self-energy of the Wilson line in the gauge invariant quasi-PDF operators causes the signal to noise ratio to decay exponentially at long distances

$$h_{\text{GI}}^{\text{B}}(z, P_z) = \langle P_z | \bar{\psi}(z) \gamma_t W(z, 0) \psi(0) | P_z \rangle \sim e^{-\delta m z}$$

- So, who needs gauge invariance anyway? In the quark case, it has been shown that (a new) factorization holds and the signal is improved at long distances at large distances when we use Coulomb gauge (CG) operators

$$h_{\text{CG}}^{\text{B}}(z, P_z) = \langle P_z | \bar{\psi}(z) \gamma_t \psi(0) |_{\nabla \cdot \vec{A}=0} | P_z \rangle$$

Gao, et al. PRD 109(0):094506 (2024)

- Rapid progress has been made for CG in the quark case (see Qi talk at 3:30pm today and Fei's at 2:30 tomorrow)

Coulomb Gauge to the Rescue

- The self-energy of the Wilson line in the gauge invariant quasi-PDF operators causes the signal to noise ratio to decay exponentially at long distances

$$h_{\text{GI}}^{\text{B}}(z, P_z) = \langle P_z | \bar{\psi}(z) \gamma_t W(z, 0) \psi(0) | P_z \rangle \sim e^{-\delta m z}$$

- So, who needs gauge invariance anyway? In the quark case, it has been shown that (a new) factorization holds and the signal is improved at long distances at large distances when we use Coulomb gauge (CG) operators

$$h_{\text{CG}}^{\text{B}}(z, P_z) = \langle P_z | \bar{\psi}(z) \gamma_t \psi(0) |_{\nabla \cdot \vec{A}=0} | P_z \rangle$$

Gao, et al. PRD 109(0):094506 (2024)

- Rapid progress has been made for CG in the quark case (see Qi talk at 3:30pm today and Fei's at 2:30 tomorrow)
- Bonus: This method makes renormalization easier and allows for direct extraction of x-space quasi-PDFs from 3pt correlators

Coulomb Gauge to the Rescue

- The self-energy of the Wilson line in the gauge invariant quasi-PDF operators causes the signal to noise ratio to decay exponentially at long distances

$$h_{\text{GI}}^{\text{B}}(z, P_z) = \langle P_z | \bar{\psi}(z) \gamma_t W(z, 0) \psi(0) | P_z \rangle \sim e^{-\delta m z}$$

- So, who needs gauge invariance anyway? In the quark case, it has been shown that (a new) factorization holds and the signal is improved at long distances at large distances when we use Coulomb gauge (CG) operators

$$h_{\text{CG}}^{\text{B}}(z, P_z) = \langle P_z | \bar{\psi}(z) \gamma_t \psi(0) |_{\nabla \cdot \vec{A}=0} | P_z \rangle$$

Gao, et al. PRD 109(0):094506 (2024)

- Rapid progress has been made for CG in the quark case (see Qi talk at 3:30pm today and Fei's at 2:30 tomorrow)
- Bonus: This method makes renormalization easier and allows for direct extraction of x-space quasi-PDFs from 3pt correlators (see Rui's talk tomorrow at 1:30pm)

Coulomb Gauge to the Rescue

- The self-energy of the Wilson line in the gauge invariant quasi-PDF operators causes the signal to noise ratio to decay exponentially at long distances

$$h_{\text{GI}}^{\text{B}}(z, P_z) = \langle P_z | \bar{\psi}(z) \gamma_t W(z, 0) \psi(0) | P_z \rangle \sim e^{-\delta m z}$$

- So, who needs gauge invariance anyway? In the quark case, it has been shown that (a new) factorization holds and the signal is improved at long distances at large distances when we use Coulomb gauge (CG) operators

$$h_{\text{CG}}^{\text{B}}(z, P_z) = \langle P_z | \bar{\psi}(z) \gamma_t \psi(0) |_{\nabla \cdot \vec{A}=0} | P_z \rangle$$

Gao, et al. PRD 109(0):094506 (2024)

- Rapid progress has been made for CG in the quark case (see Qi talk at 3:30pm today and Fei's at 2:30 tomorrow)
- Bonus: This method makes renormalization easier and allows for direct extraction of x-space quasi-PDFs from 3pt correlators (see Rui's talk tomorrow at 1:30pm)
- With this method is that matching must be recalculated for these new CG operators, which is a major challenge in the gluon case. I'll share our progress

LaMET Matching Kernel Calculation

LaMET Matching Kernel Calculation

- LaMET centers around the perturbative matching between the PDF and quasi-PDF

$$q(x, \mu^2) = \int \frac{dy}{|y|} C\left(\frac{x}{y}, \frac{\mu^2}{P_z^2}\right) \tilde{q}(y, P_z)$$

LaMET Matching Kernel Calculation

- LaMET centers around the perturbative matching between the PDF and quasi-PDF

$$q(x, \mu^2) = \int \frac{dy}{|y|} C\left(\frac{x}{y}, \frac{\mu^2}{P_z^2}\right) \tilde{q}(y, P_z)$$

- The matching kernel is calculated order by order by taking the difference between the parton-in-parton PDF and quasi-PDF

LaMET Matching Kernel Calculation

- LaMET centers around the perturbative matching between the PDF and quasi-PDF

$$q(x, \mu^2) = \int \frac{dy}{|y|} C\left(\frac{x}{y}, \frac{\mu^2}{P_z^2}\right) \tilde{q}(y, P_z)$$

- The matching kernel is calculated order by order by taking the difference between the parton-in-parton PDF and quasi-PDF

$$\tilde{q}(x, p_z) \propto \int \frac{dz}{2\pi} e^{-izxp_z} \langle q(p_z) | \bar{\psi}(z) \gamma_t W(z, 0) \psi(0) | q(p_z) \rangle$$

LaMET Matching Kernel Calculation

- LaMET centers around the perturbative matching between the PDF and quasi-PDF

$$q(x, \mu^2) = \int \frac{dy}{|y|} C\left(\frac{x}{y}, \frac{\mu^2}{P_z^2}\right) \tilde{q}(y, P_z)$$

- The matching kernel is calculated order by order by taking the difference between the parton-in-parton PDF and quasi-PDF

$$\tilde{q}(x, p_z) \propto \int \frac{dz}{2\pi} e^{-izxp_z} \langle q(p_z) | \bar{\psi}(z) \gamma_t W(z, 0) \psi(0) | q(p_z) \rangle$$

Calculable via
Feynman diagrams

LaMET Matching Kernel Calculation

- LaMET centers around the perturbative matching between the PDF and quasi-PDF

$$q(x, \mu^2) = \int \frac{dy}{|y|} C\left(\frac{x}{y}, \frac{\mu^2}{P_z^2}\right) \tilde{q}(y, P_z)$$

- The matching kernel is calculated order by order by taking the difference between the parton-in-parton PDF and quasi-PDF

$$\tilde{q}(x, p_z) \propto \int \frac{dz}{2\pi} e^{-izxp_z} \langle q(p_z) | \bar{\psi}(z) \gamma_t W(z, 0) \psi(0) | q(p_z) \rangle$$

Calculable via
Feynman diagrams

$$C^{(i)}\left(\xi = x/y, \frac{\mu^2}{p_z^2}\right) = q_q^{(i)}(\xi, p_z^2/\mu^2) - \tilde{q}_q^{(i)}(\xi, \mu^2)$$

LaMET Matching Kernel Calculation

- LaMET centers around the perturbative matching between the PDF and quasi-PDF

$$q(x, \mu^2) = \int \frac{dy}{|y|} C\left(\frac{x}{y}, \frac{\mu^2}{P_z^2}\right) \tilde{q}(y, P_z)$$

- The matching kernel is calculated order by order by taking the difference between the parton-in-parton PDF and quasi-PDF

$$\tilde{q}(x, p_z) \propto \int \frac{dz}{2\pi} e^{-izxp_z} \langle q(p_z) | \bar{\psi}(z) \gamma_t W(z, 0) \psi(0) | q(p_z) \rangle$$

Calculable via
Feynman diagrams

$$C^{(i)}\left(\xi = x/y, \frac{\mu^2}{p_z^2}\right) = q_q^{(i)}(\xi, p_z^2/\mu^2) - \tilde{q}_q^{(i)}(\xi, \mu^2)$$

- This works because, although both distributions have the same IR physics, so the IR divergence cancels out, and UV divergences can be renormalized

LaMET Matching Kernel Calculation

- LaMET centers around the perturbative matching between the PDF and quasi-PDF

$$q(x, \mu^2) = \int \frac{dy}{|y|} C\left(\frac{x}{y}, \frac{\mu^2}{P_z^2}\right) \tilde{q}(y, P_z)$$

- The matching kernel is calculated order by order by taking the difference between the parton-in-parton PDF and quasi-PDF

$$\tilde{q}(x, p_z) \propto \int \frac{dz}{2\pi} e^{-izxp_z} \langle q(p_z) | \bar{\psi}(z) \gamma_t W(z, 0) \psi(0) | q(p_z) \rangle$$

Calculable via
Feynman diagrams

$$C^{(i)}\left(\xi = x/y, \frac{\mu^2}{p_z^2}\right) = q_q^{(i)}(\xi, p_z^2/\mu^2) - \tilde{q}_q^{(i)}(\xi, \mu^2)$$

- This works because, although both distributions have the same IR physics, so the IR divergence cancels out, and UV divergences can be renormalized
- Matching to relevant lattice renormalization schemes is straightforward

Gauge Variant Gluon Quasi-PDF Operators

Gauge Variant Gluon Quasi-PDF Operators

- Since we don't care about gauge invariance anymore, we can define a new operator from the gluon fields themselves

Gauge Variant Gluon Quasi-PDF Operators

- Since we don't care about gauge invariance anymore, we can define a new operator from the gluon fields themselves

$$O^{CG}(z) = A^\perp(z)A_\perp(0)|_{\nabla \cdot \vec{A}=0}$$

Gauge Variant Gluon Quasi-PDF Operators

- Since we don't care about gauge invariance anymore, we can define a new operator from the gluon fields themselves

$$O^{CG}(z) = A^\perp(z)A_\perp(0)|_{\nabla \cdot \vec{A}=0}$$

$$\tilde{g}_H(x) = xP_z \int \frac{dz}{2\pi} e^{izxP_z} \langle H(P_z) | O^{CG}(z) | H(P_z) \rangle$$

Gauge Variant Gluon Quasi-PDF Operators

- Since we don't care about gauge invariance anymore, we can define a new operator from the gluon fields themselves

$$O^{CG}(z) = A^\perp(z)A_\perp(0)|_{\nabla \cdot \vec{A}=0}$$

$$\tilde{g}_H(x) = xP_z \int \frac{dz}{2\pi} e^{izxP_z} \langle H(P_z) | O^{CG}(z) | H(P_z) \rangle$$

- This reduces the work involved for calculating the matching significantly

Gauge Variant Gluon Quasi-PDF Operators

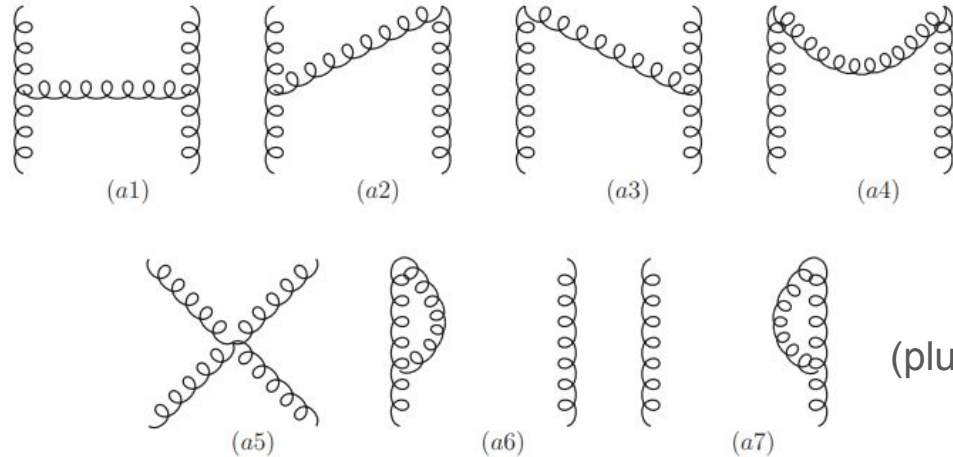
- Since we don't care about gauge invariance anymore, we can define a new operator from the gluon fields themselves

$$O^{CG}(z) = A^\perp(z)A_\perp(0)|_{\nabla \cdot \vec{A}=0}$$

$$\tilde{g}_H(x) = xP_z \int \frac{dz}{2\pi} e^{izxP_z} \langle H(P_z) | O^{CG}(z) | H(P_z) \rangle$$

- This reduces the work involved for calculating the matching significantly

Field strength tensor
NLO diagrams:



(plus self energy terms)

Gauge Variant Gluon Quasi-PDF Operators

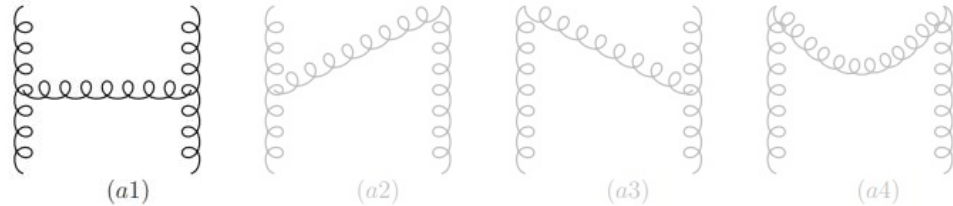
- Since we don't care about gauge invariance anymore, we can define a new operator from the gluon fields themselves

$$O^{CG}(z) = A^\perp(z)A_\perp(0)|_{\nabla \cdot \vec{A}=0}$$

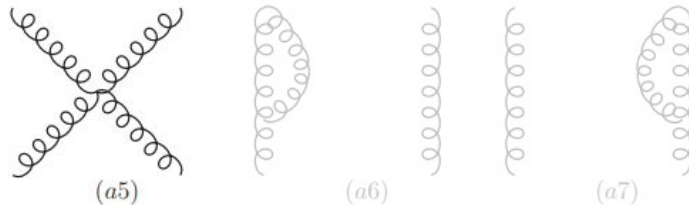
$$\tilde{g}_H(x) = xP_z \int \frac{dz}{2\pi} e^{izxP_z} \langle H(P_z) | O^{CG}(z) | H(P_z) \rangle$$

- This reduces the work involved for calculating the matching significantly

Field strength tensor
NLO diagrams:



Field correlators NLO
diagrams:



(plus self energy terms)

Wang, et al. PRD 100:074509 (2019)

Plan of Attack

Plan of Attack

- Our plan for the calculation is to use dimensional regularization (DR) with $d=4-2\epsilon$ dimensions to calculate the momentum space quasi-PDF for on-shell massless gluons

$$\tilde{g}_g(x) = xp_z \int \frac{dz}{2\pi} e^{izxp_z} \langle g(p) | O^{CG}(z) | g(p) \rangle$$

Plan of Attack

- Our plan for the calculation is to use dimensional regularization (DR) with $d=4-2\epsilon$ dimensions to calculate the momentum space quasi-PDF for on-shell massless gluons

$$p = (p_t, 0, 0, p_z)$$

$$p^2 = 0$$

$$\tilde{g}_g(x) = xp_z \int \frac{dz}{2\pi} e^{izxp_z} \langle g(p) | O^{CG}(z) | g(p) \rangle$$

Plan of Attack

- Our plan for the calculation is to use dimensional regularization (DR) with $d=4-2\epsilon$ dimensions to calculate the momentum space quasi-PDF for on-shell massless gluons

$$p = (p_t, 0, 0, p_z)$$

$$p^2 = 0$$

$$\tilde{g}_g(x) = xp_z \int \frac{dz}{2\pi} e^{izxp_z} \langle g(p) | O^{CG}(z) | g(p) \rangle$$

- We write the gluon quasi-PDF (before inclusion of crossed diagrams)

$$\tilde{g}_g^*(x) = (1 + Z_g)\delta(1 - x) + \tilde{g}_g^{(1)}(x) + \dots$$

Plan of Attack

- Our plan for the calculation is to use dimensional regularization (DR) with $d=4-2\epsilon$ dimensions to calculate the momentum space quasi-PDF for on-shell massless gluons

$$p = (p_t, 0, 0, p_z)$$

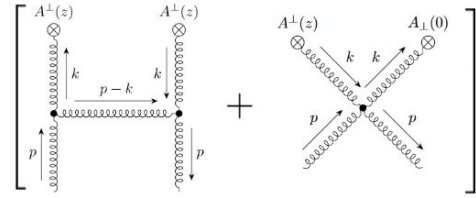
$$p^2 = 0$$

$$\tilde{g}_g(x) = xp_z \int \frac{dz}{2\pi} e^{izxp_z} \langle g(p) | O^{CG}(z) | g(p) \rangle$$

- We write the gluon quasi-PDF (before inclusion of crossed diagrams)

$$\tilde{g}_g^*(x) = (1 + Z_g)\delta(1 - x) + \tilde{g}_g^{(1)}(x) + \dots$$

$$\tilde{g}_g^{(1)}(x, p_z) = xp_z \int \frac{dz}{2\pi} e^{-ixp_z z}$$



Plan of Attack

- Our plan for the calculation is to use dimensional regularization (DR) with $d=4-2\epsilon$ dimensions to calculate the momentum space quasi-PDF for on-shell massless gluons

$$p = (p_t, 0, 0, p_z)$$

$$p^2 = 0$$

$$\tilde{g}_g(x) = xp_z \int \frac{dz}{2\pi} e^{izxp_z} \langle g(p) | O^{CG}(z) | g(p) \rangle$$

- We write the gluon quasi-PDF (before inclusion of crossed diagrams)

$$\tilde{g}_g^*(x) = (1 + Z_g)\delta(1 - x) + \tilde{g}_g^{(1)}(x) + \dots$$

$$\tilde{g}_g^{(1)}(x, p_z) = xp_z \int \frac{dz}{2\pi} e^{-ixp_z z}$$

$$Z_g = - \left. \frac{\partial \Pi_1}{\partial k^2} \right|_{k^2=0}$$

$$i\Pi^{ij}(p^2, \vec{p}^2) =$$

$$= \Pi_1(p^2, \vec{p}^2)\delta^{ij} + \Pi_2(p^2, \vec{p}^2) \frac{k^i k^j}{\vec{k}^2}$$

Plan of Attack

- Our plan for the calculation is to use dimensional regularization (DR) with $d=4-2\epsilon$ dimensions to calculate the momentum space quasi-PDF for on-shell massless gluons

$$p = (p_t, 0, 0, p_z)$$

$$p^2 = 0$$

$$\tilde{g}_g(x) = xp_z \int \frac{dz}{2\pi} e^{izxp_z} \langle g(p) | O^{CG}(z) | g(p) \rangle$$

- We write the gluon quasi-PDF (before inclusion of crossed diagrams)

$$\tilde{g}_g^*(x) = (1 + Z_g)\delta(1 - x) + \tilde{g}_g^{(1)}(x) + \dots$$

$$\tilde{g}_g^{(1)}(x, p_z) = xp_z \int \frac{dz}{2\pi} e^{-ixp_z z}$$

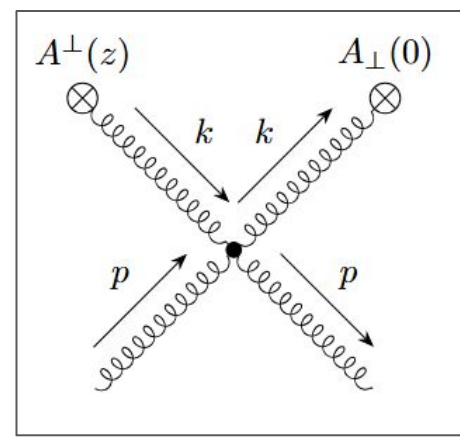
$$Z_g = - \left. \frac{\partial \Pi_1}{\partial k^2} \right|_{k^2=0}$$

$$i\Pi^{ij}(p^2, \vec{p}^2) =$$

$$= \Pi_1(p^2, \vec{p}^2)\delta^{ij} + \Pi_2(p^2, \vec{p}^2) \frac{k^i k^j}{k^2}$$

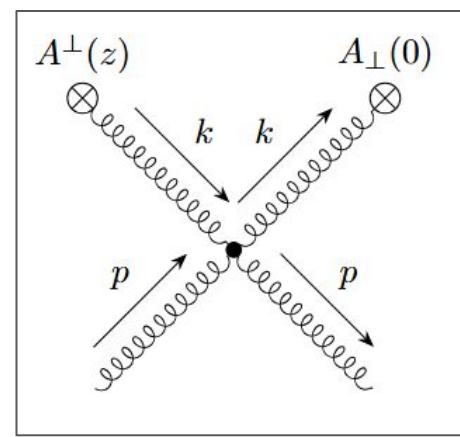
$$\tilde{g}_g(x) = \tilde{g}_g^*(x) - \tilde{g}_g^*(-x)$$

Easy Part: Four Gluon Vertex Diagram



Easy Part: Four Gluon Vertex Diagram

- The 4-gluon vertex diagram is the easier of the two

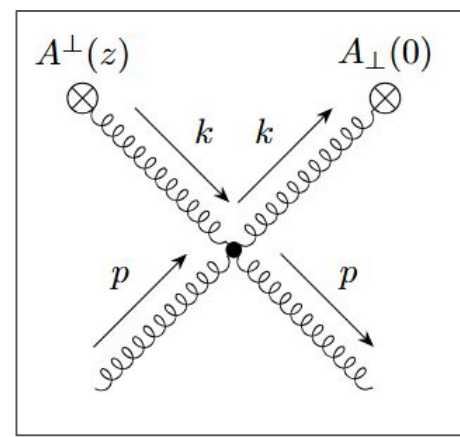


Easy Part: Four Gluon Vertex Diagram

- The 4-gluon vertex diagram is the easier of the two
- We have to deal with the CG gluon propagator which breaks symmetry in the time direction:

$$iD^{\mu\nu}(k) = \frac{-i}{k^2 + i0} \left[g^{\mu\nu} - n \cdot k \frac{n^\mu k^\nu + n^\nu k^\mu}{\vec{k}^2} + \frac{k^\mu k^\nu}{\vec{k}^2} \right]$$

$$n^\mu = (1, 0, 0, 0)$$

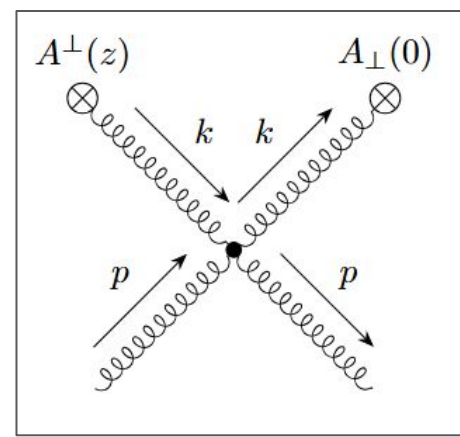


Easy Part: Four Gluon Vertex Diagram

- The 4-gluon vertex diagram is the easier of the two
- We have to deal with the CG gluon propagator which breaks symmetry in the time direction:

$$iD^{\mu\nu}(k) = \frac{-i}{k^2 + i0} \left[g^{\mu\nu} - n \cdot k \frac{n^\mu k^\nu + n^\nu k^\mu}{\vec{k}^2} + \frac{k^\mu k^\nu}{\vec{k}^2} \right]$$

$$n^\mu = (1, 0, 0, 0)$$



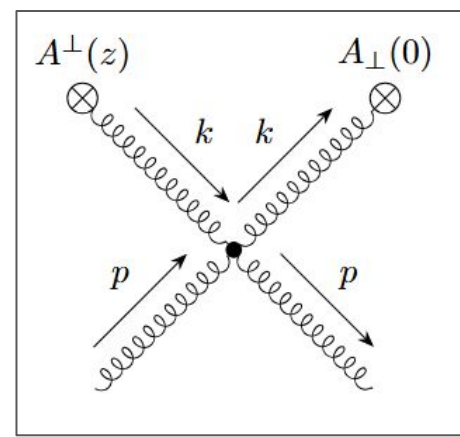
- Operator insertion plus the fourier transform results in a delta function

Easy Part: Four Gluon Vertex Diagram

- The 4-gluon vertex diagram is the easier of the two
- We have to deal with the CG gluon propagator which breaks symmetry in the time direction:

$$iD^{\mu\nu}(k) = \frac{-i}{k^2 + i0} \left[g^{\mu\nu} - n \cdot k \frac{n^\mu k^\nu + n^\nu k^\mu}{\vec{k}^2} + \frac{k^\mu k^\nu}{\vec{k}^2} \right]$$

$$n^\mu = (1, 0, 0, 0)$$



- Operator insertion plus the fourier transform results in a delta function

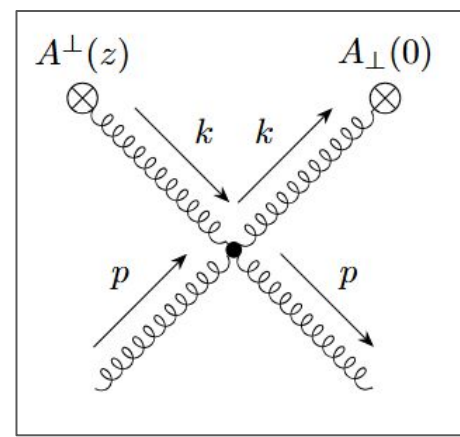
$$A_b^\mu(z) \begin{array}{c} \otimes \\ \uparrow \\ \alpha, a \end{array} = \delta^{ab} g^{\alpha\mu} e^{-ip \cdot z}$$

Easy Part: Four Gluon Vertex Diagram

- The 4-gluon vertex diagram is the easier of the two
- We have to deal with the CG gluon propagator which breaks symmetry in the time direction:

$$iD^{\mu\nu}(k) = \frac{-i}{k^2 + i0} \left[g^{\mu\nu} - n \cdot k \frac{n^\mu k^\nu + n^\nu k^\mu}{\vec{k}^2} + \frac{k^\mu k^\nu}{\vec{k}^2} \right]$$

$$n^\mu = (1, 0, 0, 0)$$



- Operator insertion plus the fourier transform results in a delta function

$$\int \frac{dz}{2\pi} \int \frac{d^d k}{(2\pi)^d} e^{-iz(k_z - xp_z)} f(k, p_z) = \int \frac{d^d k}{(2\pi)^d} \delta(k_z - xp_z) f(k, p_z)$$

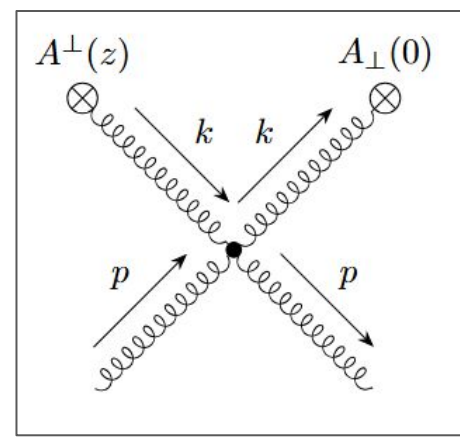
$$A_b^\mu(z) \begin{array}{c} \otimes \\ \vdots \\ \alpha, a \\ \uparrow \\ p \end{array} = \delta^{ab} g^{\alpha\mu} e^{-ip \cdot z}$$

Easy Part: Four Gluon Vertex Diagram

- The 4-gluon vertex diagram is the easier of the two
- We have to deal with the CG gluon propagator which breaks symmetry in the time direction:

$$iD^{\mu\nu}(k) = \frac{-i}{k^2 + i0} \left[g^{\mu\nu} - n \cdot k \frac{n^\mu k^\nu + n^\nu k^\mu}{\vec{k}^2} + \frac{k^\mu k^\nu}{\vec{k}^2} \right]$$

$$n^\mu = (1, 0, 0, 0)$$



- Operator insertion plus the fourier transform results in a delta function

$$\int \frac{dz}{2\pi} \int \frac{d^d k}{(2\pi)^d} e^{-iz(k_z - xp_z)} f(k, p_z) = \int \frac{d^d k}{(2\pi)^d} \delta(k_z - xp_z) f(k, p_z)$$

- We treat the temporal momentum integral as $d = 1$

$$A_b^\mu(z) \begin{array}{c} \otimes \\ \uparrow \\ \text{wavy line} \\ \alpha, a \\ \uparrow \\ p \end{array} = \delta^{ab} g^{\alpha\mu} e^{-ip \cdot z}$$

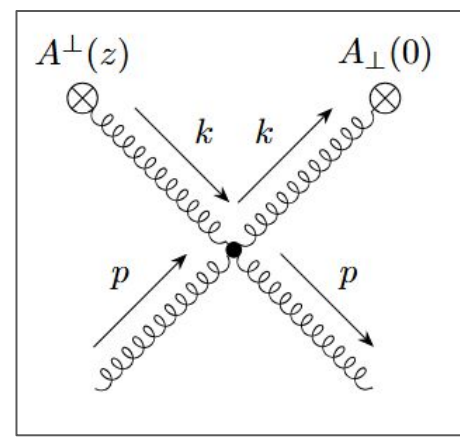
$$\int \frac{dk_t}{2\pi} \frac{1}{k^{2a}} \propto \frac{1}{k^{2(a-\frac{1}{2})}}$$

Easy Part: Four Gluon Vertex Diagram

- The 4-gluon vertex diagram is the easier of the two
- We have to deal with the CG gluon propagator which breaks symmetry in the time direction:

$$iD^{\mu\nu}(k) = \frac{-i}{k^2 + i0} \left[g^{\mu\nu} - n \cdot k \frac{n^\mu k^\nu + n^\nu k^\mu}{\vec{k}^2} + \frac{k^\mu k^\nu}{\vec{k}^2} \right]$$

$$n^\mu = (1, 0, 0, 0)$$



- Operator insertion plus the fourier transform results in a delta function

$$\int \frac{dz}{2\pi} \int \frac{d^d k}{(2\pi)^d} e^{-iz(k_z - xp_z)} f(k, p_z) = \int \frac{d^d k}{(2\pi)^d} \delta(k_z - xp_z) f(k, p_z)$$

- We treat the temporal momentum integral as $d = 1$, and then the resulting $d - 2$ Euclidean integrals are textbook

$$\int \frac{dk_t}{2\pi} \frac{1}{k^{2a}} \propto \frac{1}{k^{2(a - \frac{1}{2})}}$$

$$\int \frac{d^{d-2} \vec{k}_\perp}{(2\pi)^{d-2}} \frac{\vec{k}_\perp^{2a}}{(\vec{k}_\perp^2 + (xp_z)^2)^b}$$

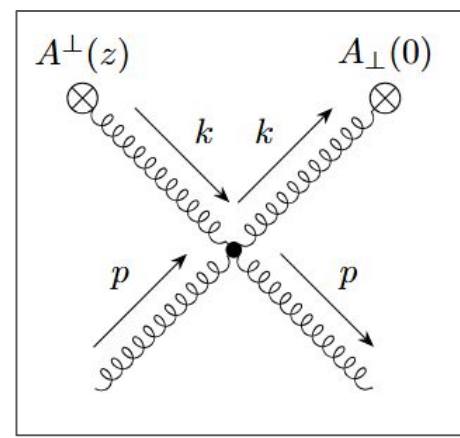
$$A_b^\mu(z) \begin{array}{c} \otimes \\ \vdots \\ \alpha, a \\ \uparrow \\ p \end{array} = \delta^{ab} g^{\alpha\mu} e^{-ip \cdot z}$$

Easy Part: Four Gluon Vertex Diagram

- The 4-gluon vertex diagram is the easier of the two
- We have to deal with the CG gluon propagator which breaks symmetry in the time direction:

$$iD^{\mu\nu}(k) = \frac{-i}{k^2 + i0} \left[g^{\mu\nu} - n \cdot k \frac{n^\mu k^\nu + n^\nu k^\mu}{\vec{k}^2} + \frac{k^\mu k^\nu}{\vec{k}^2} \right]$$

$$n^\mu = (1, 0, 0, 0)$$



- Operator insertion plus the fourier transform results in a delta function

$$\int \frac{dz}{2\pi} \int \frac{d^d k}{(2\pi)^d} e^{-iz(k_z - xp_z)} f(k, p_z) = \int \frac{d^d k}{(2\pi)^d} \delta(k_z - xp_z) f(k, p_z)$$

- We treat the temporal momentum integral as $d = 1$, and then the resulting $d - 2$ Euclidean integrals are textbook

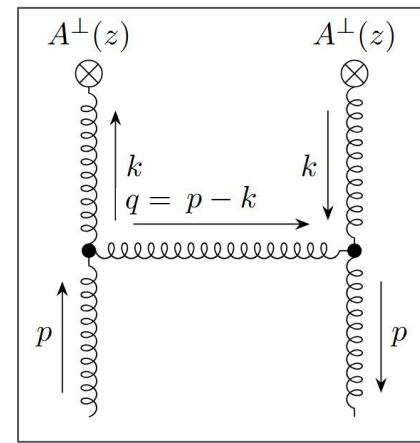
$$A_b^\mu(z) \begin{array}{c} \otimes \\ \uparrow \\ p \end{array} \alpha, a = \delta^{ab} g^{\alpha\mu} e^{-ip \cdot z}$$

$$\int \frac{dk_t}{2\pi} \frac{1}{k^{2a}} \propto \frac{1}{k^{2(a-\frac{1}{2})}}$$

$$\int \frac{d^{d-2} \vec{k}_\perp}{(2\pi)^{d-2}} \frac{\vec{k}_\perp^{2a}}{(\vec{k}_\perp^2 + (xp_z)^2)^b}$$

$$A \times \text{sgn}(x)$$

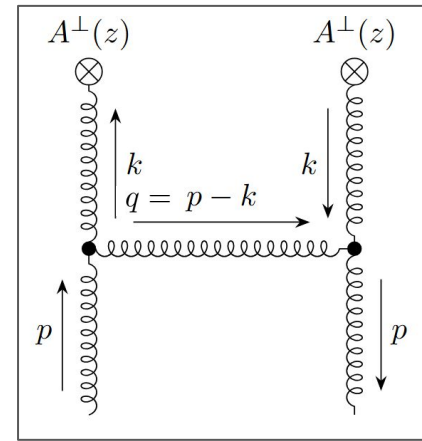
Box Diagram I



Box Diagram I

- This diagram becomes a lot harder with 3 propagators

$$\begin{aligned}
 & A g_{\perp}^{\alpha\beta} g_{\perp}^{ij} \Pi^{\gamma i}(k) \Pi^{\sigma j}(k) \Pi^{\mu\nu}(p-k) (2k^{\alpha} g^{\gamma\mu} + (p^{\mu} - k^{\mu}) g^{\alpha\gamma} + 2p^{\gamma} g^{\alpha\mu} - 2p^{\mu} g^{\alpha\gamma}) \\
 & \times (2k^{\beta} g^{\nu\sigma} + (p^{\nu} - k^{\nu}) g^{\beta\sigma} - 2p^{\nu} g^{\beta\sigma} + 2p^{\sigma} g^{\beta\nu})
 \end{aligned}$$



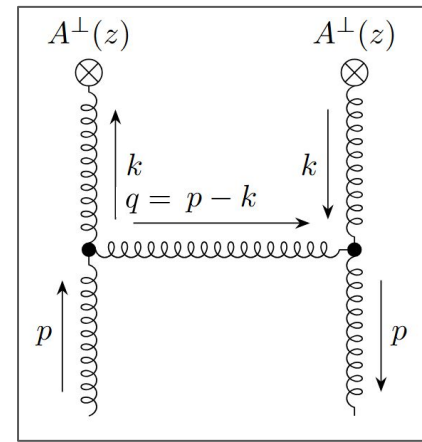
Box Diagram I

- This diagram becomes a lot harder with 3 propagators

$$A g_{\perp}^{\alpha\beta} g_{\perp}^{ij} \Pi^{\gamma i}(k) \Pi^{\sigma j}(k) \Pi^{\mu\nu}(p-k) (2k^{\alpha} g^{\gamma\mu} + (p^{\mu} - k^{\mu}) g^{\alpha\gamma} + 2p^{\gamma} g^{\alpha\mu} - 2p^{\mu} g^{\alpha\gamma})$$

$$\times (2k^{\beta} g^{\nu\sigma} + (p^{\nu} - k^{\nu}) g^{\beta\sigma} - 2p^{\nu} g^{\beta\sigma} + 2p^{\sigma} g^{\beta\nu})$$

- One can try to cleverly deal with the 16 individual contractions



Box Diagram I

- This diagram becomes a lot harder with 3 propagators

$$A g_{\perp}^{\alpha\beta} g_{\perp}^{ij} \Pi^{\gamma i}(k) \Pi^{\sigma j}(k) \Pi^{\mu\nu}(p-k) (2k^{\alpha} g^{\gamma\mu} + (p^{\mu} - k^{\mu}) g^{\alpha\gamma} + 2p^{\gamma} g^{\alpha\mu} - 2p^{\mu} g^{\alpha\gamma}) \\ \times (2k^{\beta} g^{\nu\sigma} + (p^{\nu} - k^{\nu}) g^{\beta\sigma} - 2p^{\nu} g^{\beta\sigma} + 2p^{\sigma} g^{\beta\nu})$$

- One can try to cleverly deal with the 16 individual contractions

$$T_1 = 4A g_{\perp}^{\alpha\beta} g_{\perp}^{ij} \Pi^{\gamma i}(k) \Pi^{\sigma j}(k) \Pi^{\mu\nu}(p-k) (k^{\alpha} g^{\gamma\mu}) (k^{\beta} g^{\nu\sigma}),$$

$$T_2 = 2A g_{\perp}^{\alpha\beta} g_{\perp}^{ij} \Pi^{\gamma i}(k) \Pi^{\sigma j}(k) \Pi^{\mu\nu}(p-k) (k^{\alpha} g^{\gamma\mu}) ((p^{\nu} - k^{\nu}) g^{\beta\sigma}),$$

$$T_3 = -4A g_{\perp}^{\alpha\beta} g_{\perp}^{ij} \Pi^{\gamma i}(k) \Pi^{\sigma j}(k) \Pi^{\mu\nu}(p-k) (k^{\alpha} g^{\gamma\mu}) (p^{\nu} g^{\beta\sigma}),$$

$$T_4 = 4A g_{\perp}^{\alpha\beta} g_{\perp}^{ij} \Pi^{\gamma i}(k) \Pi^{\sigma j}(k) \Pi^{\mu\nu}(p-k) (k^{\alpha} g^{\gamma\mu}) (p^{\sigma} g^{\beta\nu}),$$

$$T_5 = 2A g_{\perp}^{\alpha\beta} g_{\perp}^{ij} \Pi^{\gamma i}(k) \Pi^{\sigma j}(k) \Pi^{\mu\nu}(p-k) ((p^{\mu} - k^{\mu}) g^{\alpha\gamma}) (k^{\beta} g^{\nu\sigma}),$$

$$T_6 = A g_{\perp}^{\alpha\beta} g_{\perp}^{ij} \Pi^{\gamma i}(k) \Pi^{\sigma j}(k) \Pi^{\mu\nu}(p-k) ((p^{\mu} - k^{\mu}) g^{\alpha\gamma}) ((p^{\nu} - k^{\nu}) g^{\beta\sigma}),$$

$$T_7 = -2A g_{\perp}^{\alpha\beta} g_{\perp}^{ij} \Pi^{\gamma i}(k) \Pi^{\sigma j}(k) \Pi^{\mu\nu}(p-k) ((p^{\mu} - k^{\mu}) g^{\alpha\gamma}) (p^{\nu} g^{\beta\sigma}),$$

$$T_8 = 2A g_{\perp}^{\alpha\beta} g_{\perp}^{ij} \Pi^{\gamma i}(k) \Pi^{\sigma j}(k) \Pi^{\mu\nu}(p-k) ((p^{\mu} - k^{\mu}) g^{\alpha\gamma}) (p^{\sigma} g^{\beta\nu}),$$

$$T_9 = 4A g_{\perp}^{\alpha\beta} g_{\perp}^{ij} \Pi^{\gamma i}(k) \Pi^{\sigma j}(k) \Pi^{\mu\nu}(p-k) (p^{\gamma} g^{\alpha\mu}) (k^{\beta} g^{\nu\sigma}),$$

$$T_{10} = 2A g_{\perp}^{\alpha\beta} g_{\perp}^{ij} \Pi^{\gamma i}(k) \Pi^{\sigma j}(k) \Pi^{\mu\nu}(p-k) (p^{\gamma} g^{\alpha\mu}) ((p^{\nu} - k^{\nu}) g^{\beta\sigma}),$$

$$T_{11} = -4A g_{\perp}^{\alpha\beta} g_{\perp}^{ij} \Pi^{\gamma i}(k) \Pi^{\sigma j}(k) \Pi^{\mu\nu}(p-k) (p^{\gamma} g^{\alpha\mu}) (p^{\nu} g^{\beta\sigma}),$$

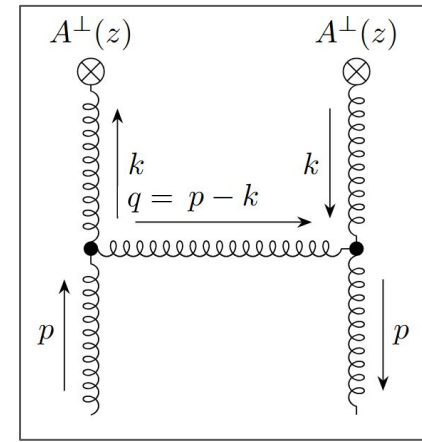
$$T_{12} = 4A g_{\perp}^{\alpha\beta} g_{\perp}^{ij} \Pi^{\gamma i}(k) \Pi^{\sigma j}(k) \Pi^{\mu\nu}(p-k) (p^{\gamma} g^{\alpha\mu}) (p^{\sigma} g^{\beta\nu}),$$

$$T_{13} = -4A g_{\perp}^{\alpha\beta} g_{\perp}^{ij} \Pi^{\gamma i}(k) \Pi^{\sigma j}(k) \Pi^{\mu\nu}(p-k) (p^{\mu} g^{\alpha\gamma}) (k^{\beta} g^{\nu\sigma}),$$

$$T_{14} = -2A g_{\perp}^{\alpha\beta} g_{\perp}^{ij} \Pi^{\gamma i}(k) \Pi^{\sigma j}(k) \Pi^{\mu\nu}(p-k) (p^{\mu} g^{\alpha\gamma}) ((p^{\nu} - k^{\nu}) g^{\beta\sigma}),$$

$$T_{15} = 4A g_{\perp}^{\alpha\beta} g_{\perp}^{ij} \Pi^{\gamma i}(k) \Pi^{\sigma j}(k) \Pi^{\mu\nu}(p-k) (p^{\mu} g^{\alpha\gamma}) (p^{\nu} g^{\beta\sigma}),$$

$$T_{16} = -4A g_{\perp}^{\alpha\beta} g_{\perp}^{ij} \Pi^{\gamma i}(k) \Pi^{\sigma j}(k) \Pi^{\mu\nu}(p-k) (p^{\mu} g^{\alpha\gamma}) (p^{\sigma} g^{\beta\nu}).$$



Box Diagram I

- This diagram becomes a lot harder with 3 propagators

$$A g_{\perp}^{\alpha\beta} g_{\perp}^{ij} \Pi^{\gamma i}(k) \Pi^{\sigma j}(k) \Pi^{\mu\nu}(p-k) (2k^{\alpha} g^{\gamma\mu} + (p^{\mu} - k^{\mu}) g^{\alpha\gamma} + 2p^{\gamma} g^{\alpha\mu} - 2p^{\mu} g^{\alpha\gamma}) \\ \times (2k^{\beta} g^{\nu\sigma} + (p^{\nu} - k^{\nu}) g^{\beta\sigma} - 2p^{\nu} g^{\beta\sigma} + 2p^{\sigma} g^{\beta\nu})$$

- One can try to cleverly deal with the 16 individual contractions

$$T_1 = 4A g_{\perp}^{\alpha\beta} g_{\perp}^{ij} \Pi^{\gamma i}(k) \Pi^{\sigma j}(k) \Pi^{\mu\nu}(p-k) (k^{\alpha} g^{\gamma\mu}) (k^{\beta} g^{\nu\sigma}),$$

$$T_2 = 2A g_{\perp}^{\alpha\beta} g_{\perp}^{ij} \Pi^{\gamma i}(k) \Pi^{\sigma j}(k) \Pi^{\mu\nu}(p-k) (k^{\alpha} g^{\gamma\mu}) ((p^{\nu} - k^{\nu}) g^{\beta\sigma}),$$

$$T_3 = -4A g_{\perp}^{\alpha\beta} g_{\perp}^{ij} \Pi^{\gamma i}(k) \Pi^{\sigma j}(k) \Pi^{\mu\nu}(p-k) (k^{\alpha} g^{\gamma\mu}) (p^{\nu} g^{\beta\sigma}),$$

$$T_4 = 4A g_{\perp}^{\alpha\beta} g_{\perp}^{ij} \Pi^{\gamma i}(k) \Pi^{\sigma j}(k) \Pi^{\mu\nu}(p-k) (k^{\alpha} g^{\gamma\mu}) (p^{\sigma} g^{\beta\nu}),$$

$$T_5 = 2A g_{\perp}^{\alpha\beta} g_{\perp}^{ij} \Pi^{\gamma i}(k) \Pi^{\sigma j}(k) \Pi^{\mu\nu}(p-k) ((p^{\mu} - k^{\mu}) g^{\alpha\gamma}) (k^{\beta} g^{\nu\sigma}),$$

$$T_6 = A g_{\perp}^{\alpha\beta} g_{\perp}^{ij} \Pi^{\gamma i}(k) \Pi^{\sigma j}(k) \Pi^{\mu\nu}(p-k) ((p^{\mu} - k^{\mu}) g^{\alpha\gamma}) ((p^{\nu} - k^{\nu}) g^{\beta\sigma}),$$

$$T_7 = -2A g_{\perp}^{\alpha\beta} g_{\perp}^{ij} \Pi^{\gamma i}(k) \Pi^{\sigma j}(k) \Pi^{\mu\nu}(p-k) ((p^{\mu} - k^{\mu}) g^{\alpha\gamma}) (p^{\nu} g^{\beta\sigma}),$$

$$T_8 = 2A g_{\perp}^{\alpha\beta} g_{\perp}^{ij} \Pi^{\gamma i}(k) \Pi^{\sigma j}(k) \Pi^{\mu\nu}(p-k) ((p^{\mu} - k^{\mu}) g^{\alpha\gamma}) (p^{\sigma} g^{\beta\nu}),$$

$$T_9 = 4A g_{\perp}^{\alpha\beta} g_{\perp}^{ij} \Pi^{\gamma i}(k) \Pi^{\sigma j}(k) \Pi^{\mu\nu}(p-k) (p^{\gamma} g^{\alpha\mu}) (k^{\beta} g^{\nu\sigma}),$$

$$T_{10} = 2A g_{\perp}^{\alpha\beta} g_{\perp}^{ij} \Pi^{\gamma i}(k) \Pi^{\sigma j}(k) \Pi^{\mu\nu}(p-k) (p^{\gamma} g^{\alpha\mu}) ((p^{\nu} - k^{\nu}) g^{\beta\sigma}),$$

$$T_{11} = -4A g_{\perp}^{\alpha\beta} g_{\perp}^{ij} \Pi^{\gamma i}(k) \Pi^{\sigma j}(k) \Pi^{\mu\nu}(p-k) (p^{\gamma} g^{\alpha\mu}) (p^{\nu} g^{\beta\sigma}),$$

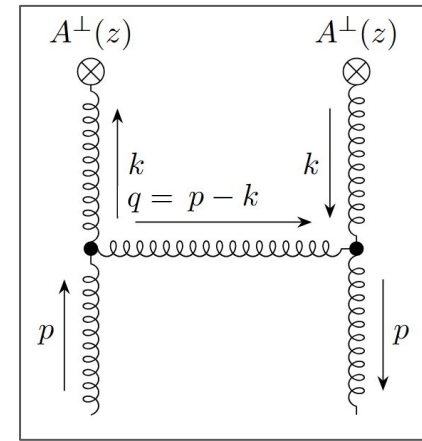
$$T_{12} = 4A g_{\perp}^{\alpha\beta} g_{\perp}^{ij} \Pi^{\gamma i}(k) \Pi^{\sigma j}(k) \Pi^{\mu\nu}(p-k) (p^{\gamma} g^{\alpha\mu}) (p^{\sigma} g^{\beta\nu}),$$

$$T_{13} = -4A g_{\perp}^{\alpha\beta} g_{\perp}^{ij} \Pi^{\gamma i}(k) \Pi^{\sigma j}(k) \Pi^{\mu\nu}(p-k) (p^{\mu} g^{\alpha\gamma}) (k^{\beta} g^{\nu\sigma}),$$

$$T_{14} = -2A g_{\perp}^{\alpha\beta} g_{\perp}^{ij} \Pi^{\gamma i}(k) \Pi^{\sigma j}(k) \Pi^{\mu\nu}(p-k) (p^{\mu} g^{\alpha\gamma}) ((p^{\nu} - k^{\nu}) g^{\beta\sigma}),$$

$$T_{15} = 4A g_{\perp}^{\alpha\beta} g_{\perp}^{ij} \Pi^{\gamma i}(k) \Pi^{\sigma j}(k) \Pi^{\mu\nu}(p-k) (p^{\mu} g^{\alpha\gamma}) (p^{\nu} g^{\beta\sigma}),$$

$$T_{16} = -4A g_{\perp}^{\alpha\beta} g_{\perp}^{ij} \Pi^{\gamma i}(k) \Pi^{\sigma j}(k) \Pi^{\mu\nu}(p-k) (p^{\mu} g^{\alpha\gamma}) (p^{\sigma} g^{\beta\nu}).$$



Only 8 of these are non-zero and unique, but it's still difficult to deal with

Box Diagram I

- This diagram becomes a lot harder with 3 propagators

$$A g_{\perp}^{\alpha\beta} g_{\perp}^{ij} \Pi^{\gamma i}(k) \Pi^{\sigma j}(k) \Pi^{\mu\nu}(p-k) (2k^{\alpha} g^{\gamma\mu} + (p^{\mu} - k^{\mu}) g^{\alpha\gamma} + 2p^{\gamma} g^{\alpha\mu} - 2p^{\mu} g^{\alpha\gamma}) \\ \times (2k^{\beta} g^{\nu\sigma} + (p^{\nu} - k^{\nu}) g^{\beta\sigma} - 2p^{\nu} g^{\beta\sigma} + 2p^{\sigma} g^{\beta\nu})$$

- One can try to cleverly deal with the 16 individual contractions

$$T_1 = 4A g_{\perp}^{\alpha\beta} g_{\perp}^{ij} \Pi^{\gamma i}(k) \Pi^{\sigma j}(k) \Pi^{\mu\nu}(p-k) (k^{\alpha} g^{\gamma\mu}) (k^{\beta} g^{\nu\sigma}),$$

$$T_2 = 2A g_{\perp}^{\alpha\beta} g_{\perp}^{ij} \Pi^{\gamma i}(k) \Pi^{\sigma j}(k) \Pi^{\mu\nu}(p-k) (k^{\alpha} g^{\gamma\mu}) ((p^{\nu} - k^{\nu}) g^{\beta\sigma}),$$

$$T_3 = -4A g_{\perp}^{\alpha\beta} g_{\perp}^{ij} \Pi^{\gamma i}(k) \Pi^{\sigma j}(k) \Pi^{\mu\nu}(p-k) (k^{\alpha} g^{\gamma\mu}) (p^{\nu} g^{\beta\sigma}),$$

$$T_4 = 4A g_{\perp}^{\alpha\beta} g_{\perp}^{ij} \Pi^{\gamma i}(k) \Pi^{\sigma j}(k) \Pi^{\mu\nu}(p-k) (k^{\alpha} g^{\gamma\mu}) (p^{\sigma} g^{\beta\nu}),$$

$$T_5 = 2A g_{\perp}^{\alpha\beta} g_{\perp}^{ij} \Pi^{\gamma i}(k) \Pi^{\sigma j}(k) \Pi^{\mu\nu}(p-k) ((p^{\mu} - k^{\mu}) g^{\alpha\gamma}) (k^{\beta} g^{\nu\sigma}),$$

$$T_6 = A g_{\perp}^{\alpha\beta} g_{\perp}^{ij} \Pi^{\gamma i}(k) \Pi^{\sigma j}(k) \Pi^{\mu\nu}(p-k) ((p^{\mu} - k^{\mu}) g^{\alpha\gamma}) ((p^{\nu} - k^{\nu}) g^{\beta\sigma}),$$

$$T_7 = -2A g_{\perp}^{\alpha\beta} g_{\perp}^{ij} \Pi^{\gamma i}(k) \Pi^{\sigma j}(k) \Pi^{\mu\nu}(p-k) ((p^{\mu} - k^{\mu}) g^{\alpha\gamma}) (p^{\nu} g^{\beta\sigma}),$$

$$T_8 = 2A g_{\perp}^{\alpha\beta} g_{\perp}^{ij} \Pi^{\gamma i}(k) \Pi^{\sigma j}(k) \Pi^{\mu\nu}(p-k) ((p^{\mu} - k^{\mu}) g^{\alpha\gamma}) (p^{\sigma} g^{\beta\nu}),$$

$$T_9 = 4A g_{\perp}^{\alpha\beta} g_{\perp}^{ij} \Pi^{\gamma i}(k) \Pi^{\sigma j}(k) \Pi^{\mu\nu}(p-k) (p^{\gamma} g^{\alpha\mu}) (k^{\beta} g^{\nu\sigma}),$$

$$T_{10} = 2A g_{\perp}^{\alpha\beta} g_{\perp}^{ij} \Pi^{\gamma i}(k) \Pi^{\sigma j}(k) \Pi^{\mu\nu}(p-k) (p^{\gamma} g^{\alpha\mu}) ((p^{\nu} - k^{\nu}) g^{\beta\sigma}),$$

$$T_{11} = -4A g_{\perp}^{\alpha\beta} g_{\perp}^{ij} \Pi^{\gamma i}(k) \Pi^{\sigma j}(k) \Pi^{\mu\nu}(p-k) (p^{\gamma} g^{\alpha\mu}) (p^{\nu} g^{\beta\sigma}),$$

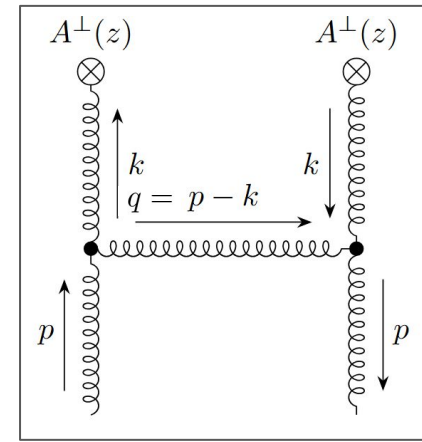
$$T_{12} = 4A g_{\perp}^{\alpha\beta} g_{\perp}^{ij} \Pi^{\gamma i}(k) \Pi^{\sigma j}(k) \Pi^{\mu\nu}(p-k) (p^{\gamma} g^{\alpha\mu}) (p^{\sigma} g^{\beta\nu}),$$

$$T_{13} = -4A g_{\perp}^{\alpha\beta} g_{\perp}^{ij} \Pi^{\gamma i}(k) \Pi^{\sigma j}(k) \Pi^{\mu\nu}(p-k) (p^{\mu} g^{\alpha\gamma}) (k^{\beta} g^{\nu\sigma}),$$

$$T_{14} = -2A g_{\perp}^{\alpha\beta} g_{\perp}^{ij} \Pi^{\gamma i}(k) \Pi^{\sigma j}(k) \Pi^{\mu\nu}(p-k) (p^{\mu} g^{\alpha\gamma}) ((p^{\nu} - k^{\nu}) g^{\beta\sigma}),$$

$$T_{15} = 4A g_{\perp}^{\alpha\beta} g_{\perp}^{ij} \Pi^{\gamma i}(k) \Pi^{\sigma j}(k) \Pi^{\mu\nu}(p-k) (p^{\mu} g^{\alpha\gamma}) (p^{\nu} g^{\beta\sigma}),$$

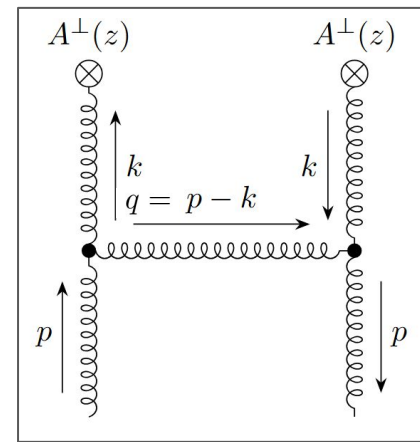
$$T_{16} = -4A g_{\perp}^{\alpha\beta} g_{\perp}^{ij} \Pi^{\gamma i}(k) \Pi^{\sigma j}(k) \Pi^{\mu\nu}(p-k) (p^{\mu} g^{\alpha\gamma}) (p^{\sigma} g^{\beta\nu}).$$



Only 8 of these are non-zero and unique, but it's still difficult to deal with

- Or we can use FeynCalc or the likes to handle these and solve the integrals algorithmically

Box Diagram II

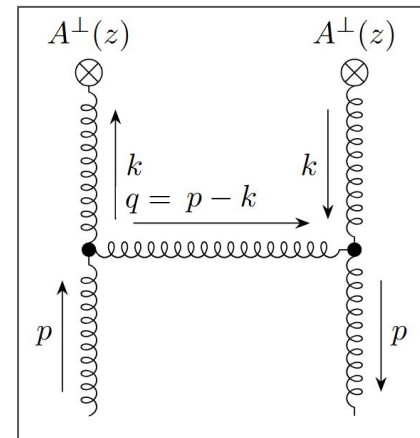


Box Diagram II

- The general form of this diagram looks like the following:

$$\int \frac{d^{D-1}k}{(2\pi)^{D-1}} \sum_i \frac{A_i(x) \vec{k}_\perp^{2n_i}}{(\vec{q}^2)^{a_i} (\vec{k}^2)^{b_i} (q^2)^{c_i} (k^2)^{d_i}}$$

$$k_z = xp_z$$



Box Diagram II

- The general form of this diagram looks like the following:

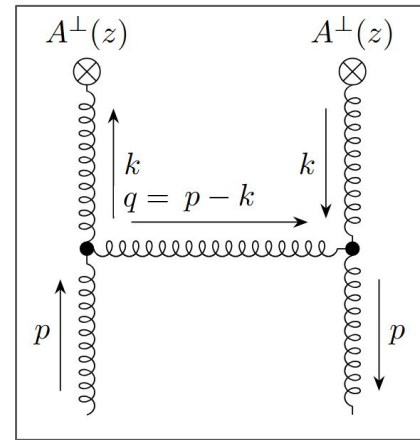
$$\int \frac{d^{D-1}k}{(2\pi)^{D-1}} \sum_i \frac{A_i(x) \vec{k}_\perp^{2n_i}}{(\vec{q}^2)^{a_i} (\vec{k}^2)^{b_i} (q^2)^{c_i} (k^2)^{d_i}}$$

$$k_z = xp_z$$

- If we do the temporal integration carefully, we can reduce everything to a nice set of $2-2\epsilon$ integrals, which have closed forms

$$\int d^{d-2} \vec{k}_\perp \frac{\vec{k}_\perp^{2n}}{(\vec{q}^2)^a (\vec{k}^2)^b} \propto G(a, b, n, d) {}_2F_1 \left(\alpha; \beta - \epsilon, \gamma; \frac{2x - 1}{x^2} \right)$$

(if a or b = 0, use textbook formula)



Box Diagram II

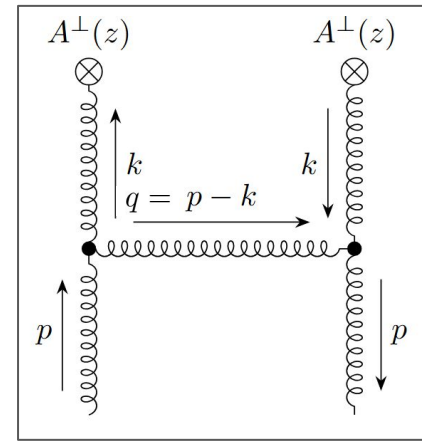
- The general form of this diagram looks like the following:

$$\int \frac{d^{D-1}k}{(2\pi)^{D-1}} \sum_i \frac{A_i(x) \vec{k}_\perp^{2n_i}}{(\vec{q}^2)^{a_i} (\vec{k}^2)^{b_i} (q^2)^{c_i} (k^2)^{d_i}} \quad \boxed{k_z = xp_z}$$

- If we do the temporal integration carefully, we can reduce everything to a nice set of 2-2 ϵ integrals, which have closed forms

$$\int d^{d-2} \vec{k}_\perp \frac{\vec{k}_\perp^{2n}}{(\vec{q}^2)^a (\vec{k}^2)^b} \propto G(a, b, n, d) {}_2F_1 \left(\alpha; \beta - \epsilon, \gamma; \frac{2x-1}{x^2} \right) \quad (\text{if } a \text{ or } b = 0, \text{ use textbook formula})$$

- The most difficult part about the rest of the calculation is handling the hypergeometric functions with parameters depending on ϵ



$$\boxed{{}_2F_1(a, b - \epsilon; c; \frac{2x-1}{x^2})} \quad \text{with } a, b, c \in \mathbb{Z}/2$$

Box Diagram II

- The general form of this diagram looks like the following:

$$\int \frac{d^{D-1}k}{(2\pi)^{D-1}} \sum_i \frac{A_i(x) \vec{k}_\perp^{2n_i}}{(\vec{q}^2)^{a_i} (\vec{k}^2)^{b_i} (q^2)^{c_i} (k^2)^{d_i}} \quad \boxed{k_z = xp_z}$$

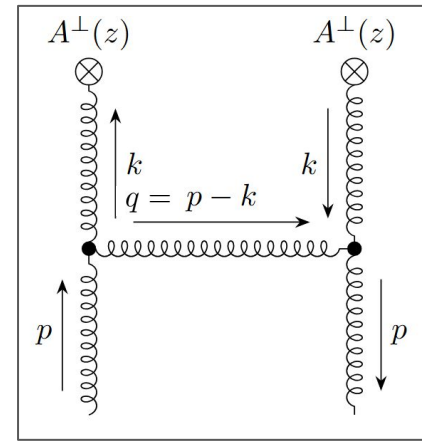
- If we do the temporal integration carefully, we can reduce everything to a nice set of 2-2 ϵ integrals, which have closed forms

$$\int d^{d-2} \vec{k}_\perp \frac{\vec{k}_\perp^{2n}}{(\vec{q}^2)^a (\vec{k}^2)^b} \propto G(a, b, n, d) {}_2F_1 \left(\alpha; \beta - \epsilon, \gamma; \frac{2x-1}{x^2} \right) \quad (\text{if } a \text{ or } b = 0, \text{ use textbook formula})$$

- The most difficult part about the rest of the calculation is handling the hypergeometric functions with parameters depending on ϵ , which hide singularities at $x=1$:

$$\boxed{{}_2F_1(a, b - \epsilon; c; \frac{2x-1}{x^2})} \quad \text{with} \quad a, b, c \in \mathbb{Z}/2$$

$$\boxed{{}_2F_1(a, b - \epsilon; c; \frac{2x-1}{x^2}) \xrightarrow{x \rightarrow 1} (1-x)^{\min[0, c-b-a+\epsilon]}}$$



ϵ -Expansion

ϵ -Expansion

Huber and Maitre, arXiv:hep-ph/0507094 and arXiv:0708.2443

- Initially, we used **HypExp** to handle the expansion of hypergeometric functions

ϵ -Expansion

Huber and Maitre, arXiv:hep-ph/0507094 and arXiv:0708.2443

- Initially, we used **HypExp** to handle the expansion of hypergeometric functions, but this does not respect expansion of terms end point singularities

$$\frac{1}{(1-x)^{1+\epsilon}} = \frac{1}{\epsilon} \delta(1-x) + \left[\frac{1}{1-x} \right]_+ + \epsilon \left[\frac{\log(1-x)}{1-x} \right]_+ + \mathcal{O}(\epsilon^2)$$

$$\int_0^1 dx [f(x)]_+ g(x) = \int_0^1 dx f(x) (g(x) - g(1))$$

ϵ -Expansion

- Initially, we used **HypExp** to handle the expansion of hypergeometric functions, but this does not respect expansion of terms end point singularities

$$\frac{1}{(1-x)^{1+\epsilon}} = \frac{1}{\epsilon} \delta(1-x) + \left[\frac{1}{1-x} \right]_+ + \epsilon \left[\frac{\log(1-x)}{1-x} \right]_+ + \mathcal{O}(\epsilon^2)$$

$$\int_0^1 dx [f(x)]_+ g(x) = \int_0^1 dx f(x) (g(x) - g(1))$$

- To handle our expansion properly, we have to isolate the singularities from the hypergeometric functions by writing:

$$\tilde{g}^{(1)}(x) = \frac{F(x, \epsilon)}{|1-x|^{1+2\epsilon}}$$

$$\tilde{F}(x, \epsilon) = \frac{F(x, \epsilon) - F(1, \epsilon)}{|1-x|^{1+2\epsilon}}$$

$$\frac{F(x, \epsilon)}{|1-x|^{1+2\epsilon}} = -\frac{F(1, \epsilon)}{2\epsilon} \delta(1-x) + F(1, \epsilon) \left[\frac{1}{|1-x|} \right]_+ - 2\epsilon F(1, \epsilon) \left[\frac{\log(1-x)}{|1-x|} \right]_+ + \tilde{F}(x, \epsilon) + \mathcal{O}(\epsilon^2)$$

ϵ-Expansion

Huber and Maitre, arXiv:hep-ph/0507094 and arXiv:0708.2443

- Initially, we used **HypExp** to handle the expansion of hypergeometric functions, but this does not respect expansion of terms end point singularities

$$\frac{1}{(1-x)^{1+\epsilon}} = \frac{1}{\epsilon} \delta(1-x) + \left[\frac{1}{1-x} \right]_+ + \epsilon \left[\frac{\log(1-x)}{1-x} \right]_+ + \mathcal{O}(\epsilon^2)$$

$$\int_0^1 dx [f(x)]_+ g(x) = \int_0^1 dx f(x) (g(x) - g(1))$$

- To handle our expansion properly, we have to isolate the singularities from the hypergeometric functions by writing:

$$\tilde{g}^{(1)}(x) = \frac{F(x, \epsilon)}{|1-x|^{1+2\epsilon}}$$

$$\tilde{F}(x, \epsilon) = \frac{F(x, \epsilon) - F(1, \epsilon)}{|1-x|^{1+2\epsilon}}$$

$$\frac{F(x, \epsilon)}{|1-x|^{1+2\epsilon}} = -\frac{F(1, \epsilon)}{2\epsilon} \delta(1-x) + F(1, \epsilon) \left[\frac{1}{|1-x|} \right]_+ - 2\epsilon F(1, \epsilon) \left[\frac{\log(1-x)}{|1-x|} \right]_+ + \tilde{F}(x, \epsilon) + \mathcal{O}(\epsilon^2)$$

- Expanding like this carefully and adding the contribution from the gluon wavefunction renormalization, we recover exactly the DGLAP kernel for our IR divergence, which nearly proves NLO factorization!

$$-\frac{P_{gg}(x)}{\epsilon_{\text{IR}}} = \frac{1}{\epsilon_{\text{IR}}} \left(-2C_A \left(\frac{x}{(1-x)_+} + x(1-x) + \frac{1-x}{x} \right) + \frac{\beta_0}{2} \delta(1-x) \right)$$

Current Results For Matching

Current Results For Matching

- For $x \neq 1$, the results look something as follows (we haven't simplified the expression with full handling of the plus prescription yet)

$$\begin{aligned}
 & \operatorname{sgn}(1-x) \left(\log(|1-x|) P_{\text{gg}}(x) + \frac{11x^6 - 34x^5 + 71x^4 - 84x^3 + 60x^2 - 24x + 4}{4(x-1)x(2x-1)^2} \right) + \\
 & \operatorname{sgn}(x) \left(\log(|x|) P_{\text{gg}}(x) + \frac{(x^4 + 4x^2 - 4x + 1)x^2 \tanh^{-1}\left(\frac{\sqrt{2x-1}}{x}\right)}{(x-1)(2x-1)^{5/2}} + \frac{90x^5 - 210x^4 + 434x^3 - 590x^2 + 357x - 74}{30(2x-1)^2x} - \right. \\
 & \left. \frac{(5x^6 - 32x^5 + 78x^4 - 120x^3 + 108x^2 - 48x + 8) \sin^{-1}\left(\frac{\sqrt{2x-1}}{x}\right)}{4(2x-1)^{5/2}x} \right) + \theta(1-x) \theta(x) P_{\text{gg}}(x) \log\left(\frac{4pz^2}{\mu^2}\right)
 \end{aligned}$$

Current Results For Matching

- For $x \neq 1$, the results look something as follows (we haven't simplified the expression with full handling of the plus prescription yet)

$$\begin{aligned} & \operatorname{sgn}(1-x) \left(\log(|1-x|) P_{\text{gg}}(x) + \frac{11x^6 - 34x^5 + 71x^4 - 84x^3 + 60x^2 - 24x + 4}{4(x-1)x(2x-1)^2} \right) + \\ & \operatorname{sgn}(x) \left(\log(|x|) P_{\text{gg}}(x) + \frac{(x^4 + 4x^2 - 4x + 1)x^2 \tanh^{-1}\left(\frac{\sqrt{2x-1}}{x}\right)}{(x-1)(2x-1)^{5/2}} + \frac{90x^5 - 210x^4 + 434x^3 - 590x^2 + 357x - 74}{30(2x-1)^2x} - \right. \\ & \left. \frac{(5x^6 - 32x^5 + 78x^4 - 120x^3 + 108x^2 - 48x + 8) \sin^{-1}\left(\frac{\sqrt{2x-1}}{x}\right)}{4(2x-1)^{5/2}x} \right) + \theta(1-x) \theta(x) P_{\text{gg}}(x) \log\left(\frac{4pz^2}{\mu^2}\right) \end{aligned}$$

- However, even after anti-symmetrizing the results, we have an issue:

$$\tilde{g}(x) \xrightarrow{|x| \rightarrow \infty} C \times \operatorname{sgn}(x) + \operatorname{sgn}(x) O(1/x^2)$$

Current Results For Matching

- For $x \neq 1$, the results look something as follows (we haven't simplified the expression with full handling of the plus prescription yet)

$$\begin{aligned}
 & \text{sgn}(1-x) \left(\log(|1-x|) P_{\text{gg}}(x) + \frac{11x^6 - 34x^5 + 71x^4 - 84x^3 + 60x^2 - 24x + 4}{4(x-1)x(2x-1)^2} \right) + \\
 & \text{sgn}(x) \left(\log(|x|) P_{\text{gg}}(x) + \frac{(x^4 + 4x^2 - 4x + 1)x^2 \tanh^{-1}\left(\frac{\sqrt{2x-1}}{x}\right)}{(x-1)(2x-1)^{5/2}} + \frac{90x^5 - 210x^4 + 434x^3 - 590x^2 + 357x - 74}{30(2x-1)^2x} - \right. \\
 & \left. \frac{(5x^6 - 32x^5 + 78x^4 - 120x^3 + 108x^2 - 48x + 8) \sin^{-1}\left(\frac{\sqrt{2x-1}}{x}\right)}{4(2x-1)^{5/2}x} \right) + \theta(1-x)\theta(x) P_{\text{gg}}(x) \log\left(\frac{4pz^2}{\mu^2}\right)
 \end{aligned}$$

- However, even after anti-symmetrizing the results, we have an issue:

$$\tilde{g}(x) \xrightarrow{|x| \rightarrow \infty} C \times \text{sgn}(x) + \text{sgn}(x) O(1/x^2)$$

- This suggests that the matching, convolution does not produce convergent results for any gluon PDF that does not approach 0 as $y \rightarrow 0$

$$\tilde{g}(x) = \int_{-1}^1 \frac{dy}{|y|} C_{gg} \left(\frac{x}{y} \right) g(y)$$

An Issue Persistent in the Literature

An Issue Persistent in the Literature

- This same behavior exists for every (gauge invariant) gluon matching kernel calculated in momentum space in the literature!

Wang EJPC 78:147, (2018)
Wang EJPC 2018, 142 (2018)
Wang PRD 100, 074509, (2019)

An Issue Persistent in the Literature

- This same behavior exists for every (gauge invariant) gluon matching kernel calculated in momentum space in the literature!

Wang EJPC 78:147, (2018)
Wang EJPC 2018, 142 (2018)
Wang PRD 100, 074509, (2019)

- This result is mentioned briefly in Balitsky, *et al.* and Yao *et al.* papers: Balitsky, et al., PLB 808:135621 (2018)
Yao, et al. JHEP 11(2023)021

This observation and the explicit expression given by Eq. (7.28) may be used to check the gluon-gluon matching kernels in Refs. [17,18]. Our check shows that $Z_1^{gg}(y, 1, p_3)|_{y>1}$ corresponding to Eq. (64) of Ref. [18] does not satisfy the constraint (7.27). The difference is by a constant term $(-2/3)$ that leads to a linear divergence in the integral of $Z_1^{gg}(y, 1, p_3)|_{y>1}$ over y . The same difference (with the opposite sign) appears in the $Z_1^{gg}(y, 1, p_3)|_{y<0}$ term in Eq. (64) of Ref. [18]. Apparently, these differences result from the use of the off-shell external gluon fields in the calculations of Ref. [18], but a discussion of this topic is outside of the scope of our paper.

because we have chosen a different Dirac structure in the quark bilinear operator. Secondly, our ratio scheme result for the unpolarized gluon PDF is in agreement with that derived in eq. (7.28) of ref. [44], which also starts from coordinate space and then Fourier transforms to momentum space. However, both the results of ref. [44] and our results show a discrepancy with earlier calculations performed directly in momentum space [43] in the unphysical region. In the ratio scheme, the contribution of the unphysical region in momentum space comes entirely from the Fourier transform of the $\ln z_{12}^2 \mu^2$ term in coordinate space. From this perspective, it is obvious that the momentum space matching in the unphysical region is entirely determined by the evolution kernel in coordinate space, where the latter is well-known in the literature. Nevertheless, it is highly desirable to further investigate and understand what leads to the mismatch between these two approaches.

An Issue Persistent in the Literature

- This same behavior exists for every (gauge invariant) gluon matching kernel calculated in momentum space in the literature!

Wang EJPC 78:147, (2018)
Wang EJPC 2018, 142 (2018)
Wang PRD 100, 074509, (2019)

- This result is mentioned briefly in Balitsky, *et al.* and Yao *et al.* papers: Balitsky, et al., PLB 808:135621 (2020)
Yao, et al. JHEP 11(2023)021

This observation and the explicit expression given by Eq. (7.28) may be used to check the gluon-gluon matching kernels in Refs. [17,18]. Our check shows that $Z_1^{gg}(y, 1, p_3)|_{y>1}$ corresponding to Eq. (64) of Ref. [18] does not satisfy the constraint (7.27). The difference is by a constant term $(-2/3)$ that leads to a linear divergence in the integral of $Z_1^{gg}(y, 1, p_3)|_{y>1}$ over y . The same difference (with the opposite sign) appears in the $Z_1^{gg}(y, 1, p_3)|_{y<0}$ term in Eq. (64) of Ref. [18]. Apparently, these differences result from the use of the off-shell external gluon fields in the calculations of Ref. [18], but a discussion of this topic is outside of the scope of our paper.

because we have chosen a different Dirac structure in the quark bilinear operator. Secondly, our ratio scheme result for the unpolarized gluon PDF is in agreement with that derived in eq. (7.28) of ref. [44], which also starts from coordinate space and then Fourier transforms to momentum space. However, both the results of ref. [44] and our results show a discrepancy with earlier calculations performed directly in momentum space [43] in the unphysical region. In the ratio scheme, the contribution of the unphysical region in momentum space comes entirely from the Fourier transform of the $\ln z_{12}^2 \mu^2$ term in coordinate space. From this perspective, it is obvious that the momentum space matching in the unphysical region is entirely determined by the evolution kernel in coordinate space, where the latter is well-known in the literature. Nevertheless, it is highly desirable to further investigate and understand what leads to the mismatch between these two approaches.

- In papers where matching is derived through position space first, this problem does not seem to occur.

A. V. Radyushkin, PRD 96:034025, 2017.
Balitsky, et al., PLB 808:135621 (2020)
Yao, et al. JHEP 11(2023)021

An Issue Persistent in the Literature

- This same behavior exists for every (gauge invariant) gluon matching kernel calculated in momentum space in the literature!

Wang EJPC 78:147, (2018)
Wang EJPC 2018, 142 (2018)
Wang PRD 100, 074509, (2019)

- This result is mentioned briefly in Balitsky, *et al.* and Yao *et al.* papers: Balitsky, et al., PLB 808:135621 (2020)
Yao, et al. JHEP 11(2023)021

This observation and the explicit expression given by Eq. (7.28) may be used to check the gluon-gluon matching kernels in Refs. [17,18]. Our check shows that $Z_1^{gg}(y, 1, p_3)|_{y>1}$ corresponding to Eq. (64) of Ref. [18] does not satisfy the constraint (7.27). The difference is by a constant term (-2/3) that leads to a linear divergence in the integral of $Z_1^{gg}(y, 1, p_3)|_{y>1}$ over y . The same difference (with the opposite sign) appears in the $Z_1^{gg}(y, 1, p_3)|_{y<0}$ term in Eq. (64) of Ref. [18]. Apparently, these differences result from the use of the off-shell external gluon fields in the calculations of Ref. [18], but a discussion of this topic is outside of the scope of our paper.

because we have chosen a different Dirac structure in the quark bilinear operator. Secondly, our ratio scheme result for the unpolarized gluon PDF is in agreement with that derived in eq. (7.28) of ref. [44], which also starts from coordinate space and then Fourier transforms to momentum space. However, both the results of ref. [44] and our results show a discrepancy with earlier calculations performed directly in momentum space [43] in the unphysical region. In the ratio scheme, the contribution of the unphysical region in momentum space comes entirely from the Fourier transform of the $\ln z_{12}^2 \mu^2$ term in coordinate space. From this perspective, it is obvious that the momentum space matching in the unphysical region is entirely determined by the evolution kernel in coordinate space, where the latter is well-known in the literature. Nevertheless, it is highly desirable to further investigate and understand what leads to the mismatch between these two approaches.

- In papers where matching is derived through position space first, this problem does not seem to occur. Unfortunately for our calculation, completing loop integration before the Fourier transform seems prohibitively difficult...

A. V. Radyushkin, PRD 96:034025, 2017.
Balitsky, et al., PLB 808:135621 (2020)
Yao, et al. JHEP 11(2023)021

An Issue Persistent in the Literature

- This same behavior exists for every (gauge invariant) gluon matching kernel calculated in momentum space in the literature!

Wang EJPC 78:147, (2018)
Wang EJPC 2018, 142 (2018)
Wang PRD 100, 074509, (2019)

- This result is mentioned briefly in Balitsky, *et al.* and Yao *et al.* papers: Balitsky, et al., PLB 808:135621 (2020)
Yao, et al. JHEP 11(2023)021

This observation and the explicit expression given by Eq. (7.28) may be used to check the gluon-gluon matching kernels in Refs. [17,18]. Our check shows that $Z_1^{gg}(y, 1, p_3)|_{y>1}$ corresponding to Eq. (64) of Ref. [18] does not satisfy the constraint (7.27). The difference is by a constant term (-2/3) that leads to a linear divergence in the integral of $Z_1^{gg}(y, 1, p_3)|_{y>1}$ over y . The same difference (with the opposite sign) appears in the $Z_1^{gg}(y, 1, p_3)|_{y<0}$ term in Eq. (64) of Ref. [18]. Apparently, these differences result from the use of the off-shell external gluon fields in the calculations of Ref. [18], but a discussion of this topic is outside of the scope of our paper.

because we have chosen a different Dirac structure in the quark bilinear operator. Secondly, our ratio scheme result for the unpolarized gluon PDF is in agreement with that derived in eq. (7.28) of ref. [44], which also starts from coordinate space and then Fourier transforms to momentum space. However, both the results of ref. [44] and our results show a discrepancy with earlier calculations performed directly in momentum space [43] in the unphysical region. In the ratio scheme, the contribution of the unphysical region in momentum space comes entirely from the Fourier transform of the $\ln z_{12}^2 \mu^2$ term in coordinate space. From this perspective, it is obvious that the momentum space matching in the unphysical region is entirely determined by the evolution kernel in coordinate space, where the latter is well-known in the literature. Nevertheless, it is highly desirable to further investigate and understand what leads to the mismatch between these two approaches.

- In papers where matching is derived through position space first, this problem does not seem to occur. Unfortunately for our calculation, completing loop integration before the Fourier transform seems prohibitively difficult...

A. V. Radyushkin, PRD 96:034025, 2017.
Balitsky, et al., PLB 808:135621 (2020)
Yao, et al. JHEP 11(2023)021

- We hope to track down some prescription to remove these singularities, we're open to suggestions

Conclusion and Outlook

Conclusion and Outlook

- We have calculated the quasi-PDF for the Coulomb gauge operator $A^\perp(z)A_\perp(0)|_{\nabla\cdot\vec{A}=0}$ via momentum space, and demonstrated that the IR behavior is the same as the light-cone PDF

Conclusion and Outlook

- We have calculated the quasi-PDF for the Coulomb gauge operator $A^\perp(z)A_\perp(0)|_{\nabla\cdot\vec{A}=0}$ via momentum space, and demonstrated that the IR behavior is the same as the light-cone PDF
- We have uncovered in our calculation, an issue with other momentum space calculations, where the matching convolution is not generally convergent

Conclusion and Outlook

- We have calculated the quasi-PDF for the Coulomb gauge operator $A^\perp(z)A_\perp(0)|_{\nabla\cdot\vec{A}=0}$ via momentum space, and demonstrated that the IR behavior is the same as the light-cone PDF
- We have uncovered in our calculation, an issue with other momentum space calculations, where the matching convolution is not generally convergent
- We plan to uncover the inconsistency between position and momentum space matching kernel calculations as a side product of this calculation

Conclusion and Outlook

- We have calculated the quasi-PDF for the Coulomb gauge operator $A^\perp(z)A_\perp(0)|_{\nabla \cdot \vec{A}=0}$ via momentum space, and demonstrated that the IR behavior is the same as the light-cone PDF
- We have uncovered in our calculation, an issue with other momentum space calculations, where the matching convolution is not generally convergent
- We plan to uncover the inconsistency between position and momentum space matching kernel calculations as a side product of this calculation
- We will also complete the more straightforward calculation of the quark-in-gluon matching once the glue-gluon calculation is resolved, though this contribution is expected to be small

Conclusion and Outlook

- We have calculated the quasi-PDF for the Coulomb gauge operator $A^\perp(z)A_\perp(0)|_{\nabla \cdot \vec{A}=0}$ via momentum space, and demonstrated that the IR behavior is the same as the light-cone PDF
- We have uncovered in our calculation, an issue with other momentum space calculations, where the matching convolution is not generally convergent
- We plan to uncover the inconsistency between position and momentum space matching kernel calculations as a side product of this calculation
- We will also complete the more straightforward calculation of the quark-in-gluon matching once the glue-gluon calculation is resolved, though this contribution is expected to be small
- We are actively measuring Coulomb gauge operators and plan to get numerical results before Lattice2026